USDRIVE

DRIVING RESEARCH AND INNOVATION FOR VEHICLE EFFICIENCY AND ENERGY SUSTAINABILITY

U.S. DRIVE Highlights of Technical Accomplishments

2015

March 2016

U.S. DRIVE
Highlights of Technical Accomplishments Overview

Through precompetitive collaboration and technical information exchange, U.S. DRIVE partners are accelerating the development and availability of clean, efficient automotive and energy technologies.

The U.S. DRIVE Partnership (*Driving Research for Vehicle efficiency and Energy sustainability*) is a voluntary government-industry partnership focused on precompetitive, advanced automotive and related infrastructure technology research and development (R&D). Partners are the United States Department of Energy (DOE); the United States Council for Automotive Research LLC (USCAR), a consortium composed of FCA US LLC (formerly Chrysler Group LLC), Ford Motor Company, and General Motors Company; Tesla Motors, Inc.; five energy companies, (BP America, Chevron Corporation, Phillips 66 Company, ExxonMobil Corporation, and Shell Oil Products US); two electric utilities, DTE Energy and Southern California Edison; and the Electric Power Research Institute.

The Partnership benefits from a history of successful collaboration across twelve technical teams, each focused on a key area of the U.S. DRIVE portfolio (see below). These teams convene the best and brightest scientists and engineers from U.S. DRIVE partner organizations to discuss key technical challenges, identify possible solutions, and evaluate progress toward goals and targets published in technology roadmaps. U.S. DRIVE also has two working groups: (1) cradle-to-grave analysis, identified as critical to better understanding the potential benefits of various technology pathways and alignment with the Partnership vision, mission, and goals; and (2) fuel properties for future engines, recognizing an important opportunity to evaluate how various fuel properties can increase the efficiency of advanced internal combustion engines. By providing a framework for frequent and regular interaction among technical experts in common areas of expertise, the Partnership accelerates technical progress, helps to avoid duplication of efforts, ensures that publicly-funded research delivers high-value results, and overcomes high-risk barriers to technology commercialization.

U.S. DRIVE technical teams selected the highlights in this document from many hundreds of DOE-funded projects conducted by some of the nation's top research organizations in the field. Each one-page summary represents what DOE and automotive, energy, and utility industry partners collectively consider to be significant progress in the development of advanced automotive and infrastructure technologies. The report is organized by technical team area, with highlights in three general categories:

Vehicles

- Advanced Combustion and Emission Control
- Electrical and Electronics
- Electrochemical Energy Storage
- Fuel Cells
- Materials
- Vehicle Systems Analysis

Crosscutting

- Codes and Standards
- Grid Interaction
- Onboard Hydrogen Storage

Fuels

- Fuel Pathways Integration
- Hydrogen Delivery
- Hydrogen Production

More information about U.S. DRIVE, including prior-year accomplishments reports and technology roadmaps, is available on the DOE (www.vehicles.energy.gov/about/partnerships/usdrive.html) and USCAR (www.uscar.org) websites.

Advanced automotive and energy infrastructure technologies are entering the market in increasing numbers, and technologies that were only concepts less than a decade ago are now approaching initial commercial readiness. These advancements are the result of partners working together to achieve a common goal. With continued progress resulting from the joint efforts of government, industry, and academic experts, the U.S. DRIVE Partnership is helping to increase the competitiveness of American industry and secure U.S. leadership in a competitive global market to enable a clean and sustainable transportation energy future.

Table of Contents

VEHICLES

Advanced Combustion and Emission Control

Experimentally Validated High-Fidelity Simulations Enable Improved Gasoline Direct Injection Fuel Injection System Designs

Detailed nozzle flow simulations revealed the mechanisms responsible for the experimentally observed differences between the angle at which injector nozzle holes are drilled and the angle of the resulting sprays.

Argonne National Laboratory

Researchers at Argonne National Laboratory have quantified the differences between the spray angle of a gasoline direct injection (GDI) injector and the angle at which the spray holes are drilled, and have discovered the mechanisms responsible for this effect using high-fidelity simulations. Correctly predicting spray characteristics is critical for GDI engine development because a desirable mixture distribution is paramount to high efficiency and low-emissions operation. A better understanding of spray characteristics improves the ability to accurately simulate and virtually optimize the combustion systems of clean-burning, highly efficient GDI engines.

High-fidelity nozzle flow simulations using high-performance computing resources show that during injection, vapor regions form in each spray hole, preferentially located near the outer edge of the nozzle (Figure 1). The volume occupied by the vapor forces the liquid fuel to flow out at a smaller angle (32°) than the angle at which the nozzle holes were drilled (37°). Further analysis revealed that as the fuel emerges from the nozzle, air entrainment in the region between the eight sprays causes a low-pressure region to develop. This further drives the sprays from all the holes to merge.

In order to validate the simulations, researchers used ultra-intense X-ray beams from the Advanced Photon Source to map the three-dimensional fuel distribution of injectors provided through the Engine Combustion Network at Sandia National Laboratories. The experiments produced highly detailed, time-resolved measurements of the fuel density in three dimensions. It was found that for each of the eight spray holes, the fuel was centered at an angle of 32° from the injector axis, confirming the prediction of the simulations.

Together, the measurements and simulations form a detailed picture of GDI fuel injection and spray formation. The advances in understanding the injection event from this work supports engine manufacturers in developing better simulation approaches, enabling accelerated design of highly efficient combustion systems.
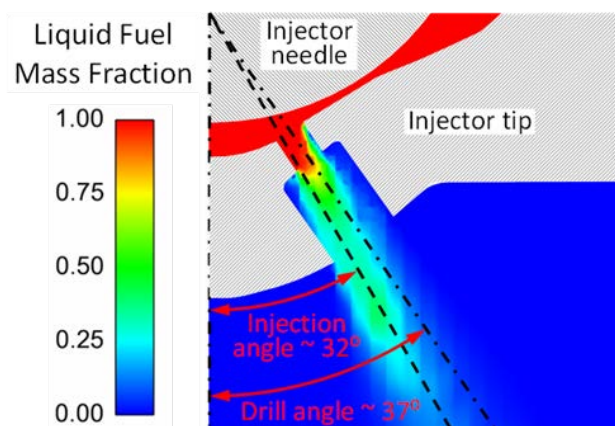
Figure 1. Computational fluid dynamics simulation of one hole in a GDI injector, showing liquid mass fraction contours. While the holes are drilled at a 37° angle from the injector axis, measurements found the sprays were directed at 32°. High-fidelity simulations reveal the flows inside the nozzle that cause this phenomenon.

Advanced Technology Light Automotive Systems Project Achieves 60% Cycle Fuel Economy Improvement over Gasoline Baseline

Advanced, aluminum block, 2.8L four-cylinder diesel engine also delivers Tier 2, Bin 2 emissions.

Cummins, Johnson Matthey, and Nissan

The ATLAS (Advanced Technology Light Automotive Systems) project has demonstrated a 60% improvement in cycle fuel economy over the baseline gasoline engine. Cummins has developed a lightweight 2.8L aluminum engine, including dual-loop exhaust gasoline recirculation (EGR), variable valve timing nitrogen oxide (NO_x) storage, and selective catalytic reduction on filter (SCRF®) catalyst systems. The engine is capable of over 220 horsepower and 425 lb-ft of torque.

Most diesel engines, regardless of application, are constructed with cast iron cylinder blocks to avoid fatigue failures due to high-cylinder pressure that puts the block in tension. While the iron can avert the fatigue failures, the weight penalty is severe. Cummins' design includes an "iron sandwich," in which an iron ladder frame and cam carrier capture the aluminum block and cylinder head by threading thru-bolts, connecting iron to iron. This construction reduced the weight of a conventional all-iron engine by over 50 kg while still providing cylinder pressure capability over 200 bar. This system allowed the full vehicle assembly with diesel-necessary peripherals included to match the weight of the baseline all-aluminum 5.6L V-8 gasoline engine.

The new engine is equipped with a variable valve timing system that allows one intake valve to follow alternate lift patterns. This technology was chosen to create high swirl conditions for improved combustion under light load driving conditions, yielding low engine-out particulate matter emissions. When the load demand is increased, the alternate pattern allows for increased lift and duration, hence increased air flow with lower swirl for higher output.

The dual loop, high-pressure (uncooled) and low-pressure (cooled) EGR system was employed to reduce the engine-out NO_x without negatively affecting fuel consumption. The separate legs of the

EGR system are controlled to meet a targeted intake manifold oxygen concentration. For most conditions, both loops operate simultaneously. This EGR system is a significant contributor to fuel economy improvement, second only to the high expansion ratio afforded by the diesel combustion system. Finally, displacement downsizing also contributes to the overall fuel economy improvement.

The aftertreatment system used Johnson Matthey's diesel cold start concept (dCSC®) and SCRF® technology. The dCSC® captured 100% of the NO_x emissions for the first 70 seconds of operation, when the downstream SCRF® was too cold to reduce NO_x. As the dCSC® starts to release NO_x, the SCRF® is approaching high conversion temperatures, only allowing 0.2 grams total NO_x emission from the tailpipe in bag 1. Due to limitations of the project, a gaseous ammonia system was used for reductant, so that mixing and fouling did not hamper results. As shown in Table 1, the system as tested on federal test procedure (FTP) and highway fuel economy test (HFET) delivered 60% improved corporate average fuel economy (CAFE) results over the baseline while meeting Tier 2, Bin 2 tailpipe emissions.

Data in MPG	Baseline Gasoline V8	DoE Program Targets	ATLAS Demo	% Improvement
FPT-75	15.6	21.8	26.0	67%
HFET	24.5	34.3	36.2	48%
CAFE weighted	18.6	26.0	29.8	60%

Table 1. Vehicle test results on FTP-75 and highway cycles.

Radio Frequency Sensor Feedback Reduces Fuel Used for Diesel Particulate Filter Regeneration

Advanced radio-frequency sensors enable optimized particulate filter management to reduce fuel consumed for soot oxidation allowing for more efficient engine and emissions aftertreatment system operation.

Filter Sensing Technologies Inc., Oak Ridge National Laboratory, Corning Incorporated, Daimler Trucks North America, FEV, and the City of New York Department of Sanitation

Filter Sensing Technologies (FST) has developed and demonstrated radio frequency (RF) sensors based on low-cost circuit chips now widespread in mobile phones and wireless networks to provide accurate measurements of particulate filter loading. Diesel particulate filters (DPF) are used on nearly all diesel engines (light duty and heavy duty) to meet particulate matter (PM) emissions limits, but filter status is estimated only indirectly using differential pressure (ΔP) sensors. The indirect ΔP measurement results in more frequent and longer regenerations, which increase fuel consumption. In contrast, RF sensors transmit a signal through the filter that directly measures the soot and ash accumulation on the filter. The approach offers a more accurate measurement of DPF loading, which can help eliminate unnecessary DPF regenerations and thereby decrease the regeneration fuel penalty.

Figure 1 shows the estimated reduction in DPF-related fuel penalty relative to the current baseline, achieved by (1) extending the time between regenerations and (2) reducing the time of each regeneration at a given soot load using the RF sensors. Conventional (ΔP) sensors also suffer from errors induced by backpressure associated with ash build-up (3) in Figure 1, which results in increased regeneration frequency as the filter ages. The results are based in part on work that Oak Ridge National Laboratory conducted on a 1.9L General Motors turbo-diesel engine demonstrating fast-response measurements of the filter loading state, which provides direct feedback control to reduce the fuel consumption associated with DPFs.

In addition, fleet testing on New York City sanitation trucks and engine dynamometer testing with FEV utilizing a model year 2013 DD-13 engine Daimler Trucks North America provided has also confirmed

the potential to extend the time between filter regenerations and decrease the regeneration duration using the RF sensor. Parallel testing at Corning and FST have further evaluated the RF sensor accuracy in the presence of ash with aged filters. Depending on the drive cycle (urban/highway) and regeneration strategy, fuel savings of 0.5% to 2% over the life of the filter are possible (Figure 1).
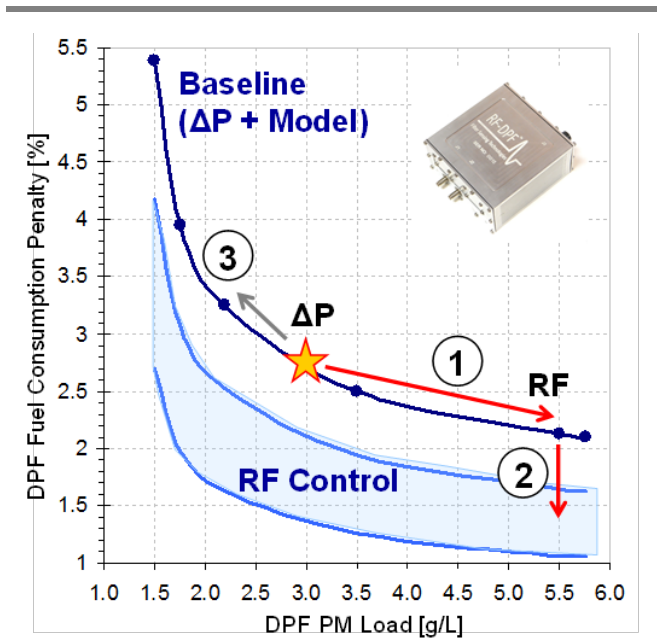
Figure 1. DPF-related fuel savings enabled by RF sensing via: (1) extended regeneration intervals, (2) shorter regenerations, and (3) absence of ash-induced error on the RF sensor response to soot.

Advanced Gasoline Turbocharged Direct Injection Engine Development Achieved 25% Fuel Economy Improvement and Met SULEV30 Emissions

Efficiency improved by engine downsizing, advanced dilute combustion, advanced boosting, and cooling systems, friction reduction, engine controls, and NVH countermeasures.

Ford Motor Company and Michigan Technological University

Ford Motor Company, with support from Michigan Technological University on advanced ignition, achieved a 25% fuel economy improvement in a mid-sized sedan using an advanced gasoline turbocharged direct injection (GTDI) engine (Figure 1). The vehicle simultaneously met super ultra-low emission vehicle (SULEV) 30 emissions standards with full useful life catalysts and no gasoline particulate filter on the Federal Test Procedure (FTP)-75 cycle (Figure 2). The measured fuel economy improvement was 25% relative to the 3.5L V6 baseline, the measured emissions were non-methane organic gasses (NMOG) plus nitrogen oxide (NO_x) at 25 mg/mile, and particulate matter (PM) at 1 mg/mile, relative to the 30 mg/mile and 3 mg/mile standards, respectively. The fuel economy and emissions results included Bags 1, 2, 3 and Highway.

The fuel economy improvements were the result of 1) aggressive engine downsizing from a 3.5L V6 to a 2.3L I4; 2) low-pressure, cooled exhaust gas recirculation; 3) a twin scroll turbocharger with an active scroll control and an active wastegate; 4) a variable displacement oil pump and roller bearing cam journals; 5) engine stop/start controls; and 6) a torque converter pendulum damper and active powertrain mounts. The transverse central direct injection combustion system met SULEV30 standards for NMOG+NO_x and PM emissions.

Figure 2. Vehicle on FTP-75 cycle.

Calibrating low-pressure, cooled exhaust gas recirculation was challenging due to dilute combustion limits, internal and external dilution controls, and exhaust gas recirculation schedule constraints, as was calibrating torque converter lock schedule, transmission shift schedule, and other vehicle level features. These challenges were met, and vehicle level integration was successful in realizing the technology benefits and achieving all project objectives.

Figure 1. 2.3L I4 advanced GTDI engine.

Novel Sensor Tracks Nitrogen Oxide and Hydrocarbon Emissions for Improved On-Board Diagnostics of Diesel Engines

Tunable selectivity of versatile sensor technology has the potential to provide feedback control from both nitrogen oxide and hydrocarbon gas species.

Los Alamos National Laboratory and Oak Ridge National Laboratory

Novel sensor technologies are required to go beyond the limitations of current commercial sensors and enable advanced combustion and emission control for fuel-saving lean-burn and low-temperature combustion engines. Los Alamos National Laboratory (LANL) has developed a sensor that can measure both nitrogen oxide (NO_x) and hydrocarbon (HC) emissions for application in on-board diagnostics and emissions control; the sensor has demonstrated stability and sensitivity in bench-scale lab testing. The sensor design was recently evaluated under diesel engine exhaust conditions at Oak Ridge National Laboratory's National Transportation Research Center through a collaborative effort.

A single LANL sensor with this design can measure both NO_x and HCs independently in diesel exhaust by simply changing the sensor's mode of operation. The electrochemical sensor design is derived from the ubiquitous zirconia-based automotive lambda sensor, but incorporates uniquely designed electrodes and solid electrolyte that permit the device to respond independently to both NO_x and HC species. This design yields a robust electrochemical interface, and offers stability needed for lifetime requirements. Most significant is the ability to shift the preferential selectivity of the device from HC to NO_x species by simply applying a small direct current electric current bias.

The sensor response correlates well with NO_x and HC concentrations (when operated in the respective sensing mode) measured via a standard laboratory Fourier transform infrared instrument under transient engine operation. Additionally, researchers obtained quantitative correlation to laboratory calibrations under steady engine load while varying exhaust gas recirculation levels (Figure 1). The sensor responses to HCs and varying ratios of $NO:NO_2$ were used to develop calibration curves. Researchers then used these calibration curves to calculate the concentration of these species from the sensor voltage response during the dynamometer experiments. The capability to measure NO_x and HCs will enable feedback control for engine and emission control technologies to help advanced combustion engines meet stringent new U.S. Environmental Protection Agency Tier 3 emission regulations.
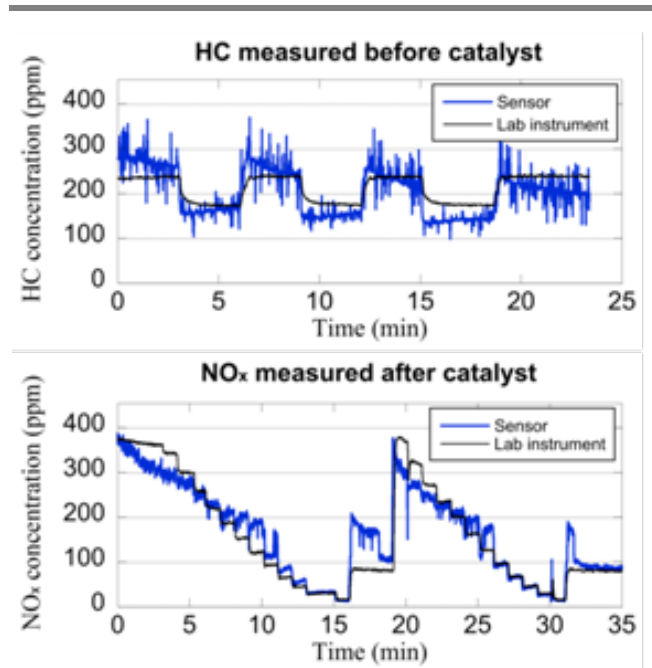
Figure 1. Top: Sensor operating in HC sensing mode upstream of catalyst. Bottom: The same sensor operating in NO_x sensing mode downstream of catalyst. Both plots compare the concentration of HC/NO_x measured via a lab standard instrument to that calculated from HC/NO_x sensor response.

High-Octane Fuel Formulations Offer Opportunities for Improving Engine Efficiency

Studies show that heat-of-vaporization changes do not affect engine efficiency for fixed octane sensitivity.

Oak Ridge National Laboratory

Fuel heat-of-vaporization (HoV) has gained attention for the potential knock-resistance benefits offered in direct-injection engines as a result of including ethanol in gasoline. Improving knock resistance of fuel is a near-term pathway to providing greater engine efficiency. Oak Ridge National Laboratory (ORNL) studies of high-octane fuels to enable increases in engine efficiency have shown that the anti-knock performance of three different fuel blends with closely-matched research octane number (RON) and motor octane number (MON) are very similar, despite differences in the latent HoV for the three fuels.

RON and MON are averaged to calculate the anti-knock index, which is posted on refueling pumps and is familiar to most consumers. Research has shown that the RON is now the most relevant rating for most light-duty engines. Sensitivity, the difference between RON and MON, has also been shown to be important in modern engines. Ethanol blending increases RON and additionally increases HoV, which may offer further anti-knock benefits along with RON and sensitivity.

ORNL used three premium-grade fuels with well-matched RON and MON ratings to evaluate the potential impact of HoV on engine efficiency. The fuels were produced using different blending streams (ethanol, isobutanol, and toluene) so that their HoV values were divergent. These fuels were evaluated across the available range of engine output torque at a fixed speed of 2,000 revolutions per minute (RPM). Marginal differences in anti-knock performance of these fuels were observed to trend with the slight differences in the RON rating of the fuels, with no additional benefit from HoV observed. Despite having a lower HoV, the toluene-blended fuel required the least combustion phasing delays to avoid knock, consistent with its slightly higher RON

rating compared with the other two fuels. As a result of their similar anti-knock performance, these fuels demonstrated similar engine efficiency. This study, in combination with results from other studies, affirms that varying HoV in the absence of a change in RON or sensitivity does not affect engine efficiency.
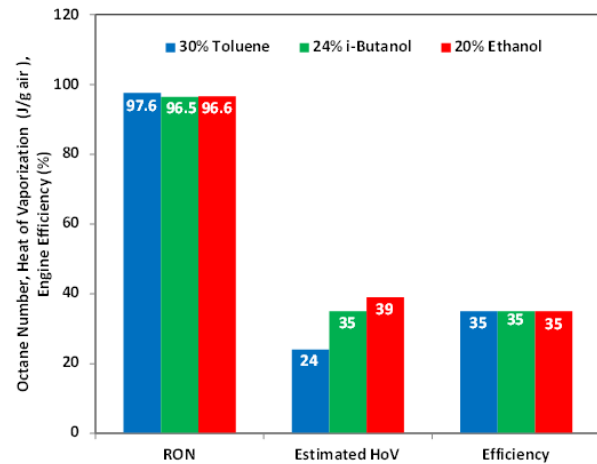
Figure 1. Three fuels with well-matched RON and differing HoV produced the same maximum fuel efficiency at 2,000 RPM.

Innovative Metal Oxide Catalyst Improves Low-Temperature Reactivity of Traditional Oxidation Catalyst

A recently discovered catalyst enables traditional precious metal-based catalysts to oxidize hydrocarbons at lower temperatures, thereby improving the production viability of advanced fuel-efficient engines.

Oak Ridge National Laboratory

A new metal oxide catalyst developed at Oak Ridge National Laboratory (ORNL) improves low-temperature performance when combined with traditional precious metal-based catalysts. The improved oxidation of hydrocarbons (HC) and carbon monoxide (CO) this new catalyst achieves addresses challenges created by advanced combustion engines, which have lower exhaust temperatures. Controlling emissions at the lower temperatures is necessary to enable advanced fuel-saving engines to be production viable.

Precious metal, specifically platinum (Pt)-group metal, catalysts are the current standard for pollutant control in lean engine exhaust because of their excellent oxidation performance and durability. However, Pt catalysts are susceptible to inhibition at low temperatures, which is problematic for use with advanced combustion engines. Inhibition occurs when one pollutant covers the active catalyst sites, which blocks access to active sites by other pollutant species and thereby prevents oxidation of the second pollutant. Of particular concern is the inhibition between CO and HC species because both CO and HC emissions tend to increase for advanced combustion engines.

ORNL has developed a ternary mixed oxide catalyst composed of copper oxide, cobalt oxide, and ceria (dubbed CCC) to facilitate low-temperature oxidation. In the powder form, the innovative CCC catalyst outperforms Pt catalysts for CO oxidation in simulated exhaust streams on a bench flow reactor. Although CCC is not as effective as a Pt catalyst for HC oxidation, when combined with a Pt catalyst, the CCC's high CO conversion can reduce the inhibition problem for the Pt catalyst and improve the overall low-temperature HC conversion.

Figure 1 shows HC performance curves comparing the CCC+Pt catalyst to a Pt-based catalyst. The Pt catalyst is on an aluminum oxide support, and the CCC+Pt catalyst is a physical mixture of the two catalysts. The study was conducted with simulated exhaust containing the criteria engine pollutants nitric oxide, CO, and HCs; here, propene (C_3H_6) is the specific HC conversion shown. Oxygen, carbon dioxide, and water are also present to accurately represent the lean engine exhaust. The Pt catalyst by itself oxidizes 90% of the C_3H_6 by 265°C (T_{90}), but the combination of the CCC and Pt catalyst achieves 90% conversion at 240°C. This new catalyst has great potential as a production-viable component in emission control systems for advanced combustion engines with low-temperature exhaust.
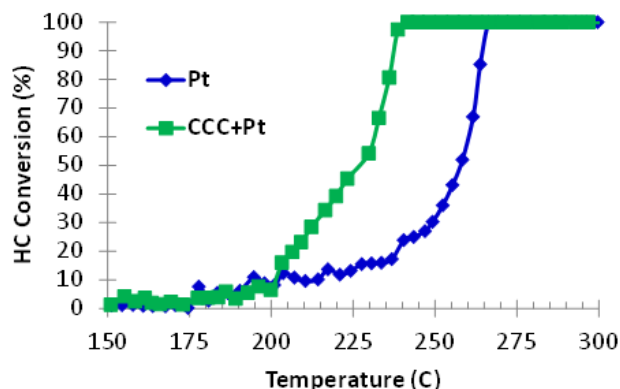
Figure 1. HC conversion in simulated exhaust using a physical mixture of the CuO_x-CoO_y-CeO_2 (CCC) and Pt catalysts as compared with the standard Pt catalyst alone. Results illustrate that CCC improves the HC conversion performance in the combined system.

Promising Automotive Catalyst Provides Nitrogen Oxide Control at Temperatures Approaching 150°C

A new selective catalytic reduction catalyst shows 90% NO_x conversion at temperatures significantly lower than current technology, which may help high-efficiency lean-burn engines satisfy SULEV30 emissions requirements.

Pacific Northwest National Laboratory

A new automotive catalyst has been developed at Pacific Northwest National Laboratory (PNNL) that may enable future high-efficiency vehicles. Lean combustion gasoline and diesel engines provide substantially higher fuel efficiency, reduced carbon dioxide emissions, and performance rivaling that of stoichiometric gasoline engines. However, meeting stringent U.S. Environmental Protection Agency Tier 3 and LEVIII emissions standards using these higher-efficiency engines continues to be a major challenge. This new catalyst for the selective catalytic reduction (SCR) of nitrogen oxide (NO_x), employing either upstream ammonia (NH_3) injection or passive NH_3 generation, is a promising innovation for controlling NO_x in a manner that helps meet relevant emissions standards.

In addition to regulating emission levels, current standards also mandate that aftertreatment systems must be durable up to 150,000 miles of use for commercialization. Discovering and developing materials and emissions systems that are able to attain these in-use requirements is a daunting task. Researchers at PNNL, however, have developed a class of novel SCR catalysts that may satisfy these prerequisites. This SCR technology, based on the industry standard Cu/SSZ-13 but with additional alkali or alkaline earth co-cations, provides increased NO_x conversion efficiency at lower exhaust temperatures more typically encountered with higher-efficiency engines.

An appropriate measure of low-temperature activity is the so-called T-90, measured as part of a performance "light-off" curve. Such curves measure the conversion of a reactant (NO_x in this case) as a function of temperature, and T-90 is the temperature at which conversion is 90%. As shown in Figure 1, while the T-90 for the industry standard catalyst, Cu/SSZ-13, is ~205°C, a newly discovered

formulation has a significantly lower T-90 of ~185°C. Although T-90s for both the industry standard and the new catalyst formulations increase slightly after exposure to an industry-established accelerated aging procedure, simulating aging effects on a vehicle, the new material shows remarkable resilience.

This new material is being further improved to meet industry needs for conversion efficiencies of 90% at 150°C, while also maintaining sufficient durability to meet regulatory requirements. Real-world application of low-temperature SCR systems could require new NH_3 delivery methods, which are also the subject of current research at PNNL.
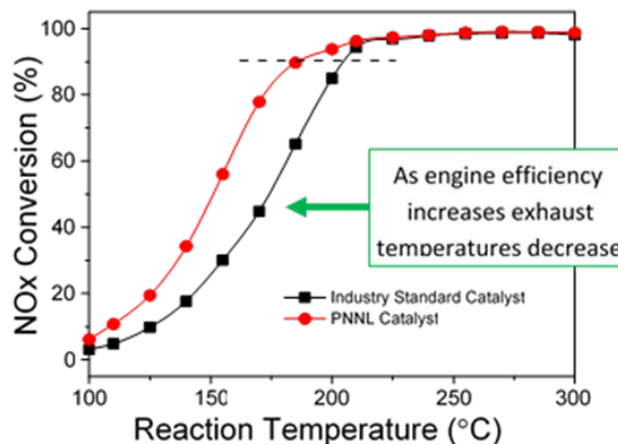
Figure 1. NO_x conversion efficiency during NH_3 SCR with a novel catalyst formulation developed and tested at PNNL. Test conditions include surrogate vehicle exhaust components.

First Principles Simulations Reveal Details of Fuel Injection that Control Combustion and Emissions

Results quantify the dominating effects of fine-scale transient fuel-air mixing and turbulence on ignition and combustion performance with unprecedented fidelity.

Sandia National Laboratories

Traditional computational models for fuel injection do not provide the level of spatial or temporal fidelity required to capture the detailed turbulent mixing, thermodynamics, and transport processes that lead to ignition and combustion in diesel engines. These highly simplified models require significant calibration, which limit their ability to accurately predict behavior in new engine designs. While experiments provide some of the data required for model improvement and validation, additional information is required to fully quantify the localized transient three-dimensional interactions between processes.

To provide this information, researchers performed a series of one-of-a-kind simulations using large eddy simulation (LES). LES directly resolves important turbulence and fuel-air mixing processes in a flow, facilitating detailed studies of strongly coupled physics at actual engine operating conditions. The unique massively-parallel solver used for these simulations employs first principles sub-models that operate within a fully coupled representation of the governing conservation equations, while running efficiently on the fastest and largest high-performance supercomputers within the U.S. Department of Energy complex.

Figure 1 shows a typical result, which is a three-dimensional rendering of a fuel jet at typical diesel engine operating conditions. The fuel is injected from left to right from the injector nozzle at 363°K into air at 6 MPa and 900°K. The red iso-surface emanating from the nozzle marks the central liquid core where large density gradients exist. These gradients induce high shear forces through strongly coupled interactions between turbulence, transport of mass and energy, and non-ideal gas-liquid thermodynamics. Instabilities form in these regions, creating flow structures that entrain air and generate intense turbulence. These structures are shown in Figure 1 by the yellow to blue iso-surfaces that begin just downstream of the central liquid core. Molecular diffusion completes the mixing, as shown by the more diffuse nature of the temperature field in the lower panel. Simultaneously, transonic velocities create large pressure fluctuations (rear panel) that couple with the density gradients to modify the flow. These complex dynamics cannot be characterized experimentally or reproduced with existing industry models or codes.
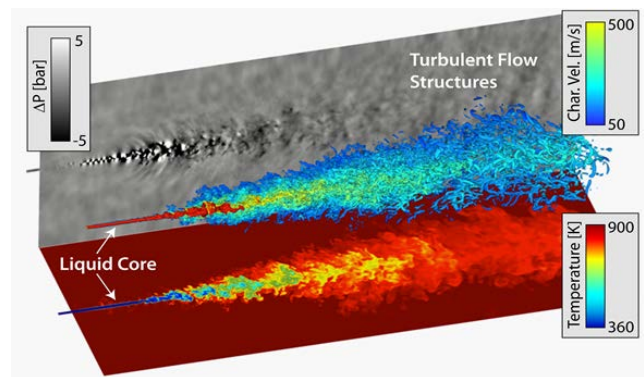
Figure 1. Three-dimensional rendering of transient fuel injection processes showing intense turbulence and resultant transient pressure (back plane) and temperature (bottom plane) fields.

The spatial and temporal fidelity of these calculations captures the fine-scale processes that directly impact fuel-air mixing, and provide the quantitative data necessary to develop the improved, affordable engineering models needed for engine design and optimization.

Mechanism for Stabilizing Fuel-Efficient, Stratified Spark Ignition Operation Identified

Multi-hole fuel sprays enhance intake-generated swirl and reduce flow variability near the spark.

Sandia National Laboratories

Research at Sandia National Laboratories has clarified the mechanism by which intake-generated swirl promotes stable combustion in stratified-charge spark-ignition (SI) engines operated on gasoline or mid-level ethanol blends. Low-combustion variability leading to stable, smooth operation is essential for fuel-efficient engines to gain market acceptance. Using an optically-accessible engine, in-cylinder flow was examined with particle image velocimetry for swirling and non-swirling flows. Measurements show that swirl makes flow patterns of individual cycles more similar to the ensemble-averaged cycle. This effect is quantified statistically through a flow similarity parameter (R_p), and shows that operation with swirl increases R_p from 0.77 to 0.90 at the time of spark ignition, reducing piston-work variability from 3.5% to 1.4% (Figure 1).

The interaction of the eight fuel sprays with the swirling gas flow strongly contributes to the flow stabilization at the time and location of the spark (Figure 1). The flow measurements reveal that the fuel sprays displace low-angular momentum gas downwards. In the wake of the spray, higher angular momentum gas from larger radii flows inward and increases its rotation rate due to conservation of momentum. This process creates a strong and very repeatable vortex near the spray centerline at the time of spark, as demonstrated by the vector fields on the right-hand-side of Figure 2. The increased flow similarity stabilizes the combustion process by reducing variability in both the ignition event and in the flame spread throughout the remaining charge. This avoids the occurrence of slow-burning cycles that may develop into partial burns. In contrast, the flow fields without swirl (Figure 2, left) show no evidence of such a stabilizing vortex. Moreover, the single-cycle example without swirl is quite different

from the average flow field, consistent with the observed higher combustion variability.

This understanding of swirl-spray interactions allows combustion engineers to optimize injector and flow parameters to maximize combustion stability and enable highly efficient stratified-charge SI operation.
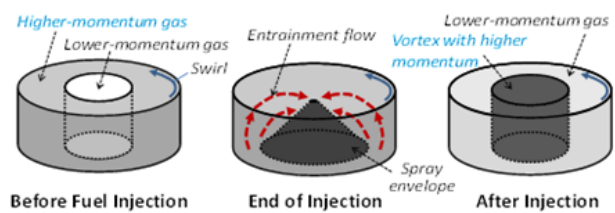
Figure 1. Conceptual model of spray-swirl interactions that create a repeatable vortex near the spark plug.
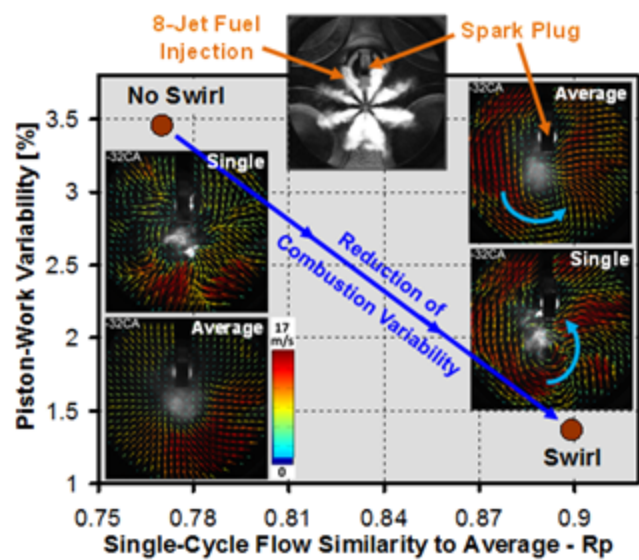
Figure 2. Effect of swirl on combustion and flow variability.

Electrical and Electronics

General Motors' Next-Generation Inverter Approaches U.S. Department of Energy's 2020 Goals

General Motors developed, tested, and demonstrated a scalable and highly efficient inverter that meets DOE's 2020 power density targets and is projected to meet DOE's 2020 cost target at a scaled-up power level.

General Motors LLC

General Motors LLC's (GM) next-generation inverter achieved the U.S. Department of Energy's (DOE) 2020 traction inverter power density target of 13.4 kW/L and specific power target of 14.1 kW/kg. If GM's internal cost targets for the components and other manufacturing targets are achieved, the next-generation inverter is projected to meet DOE's 2020 cost target of $3.30/kW if scaled up to its maximum power level (significantly higher than the 55 kW the DOE targets were based on) with 100,000 units of annual volume.

In this project, GM collaborated with Oak Ridge National Laboratory, the National Renewable Energy Laboratory, and other technology and equipment suppliers.

The performance of the inverter prototype (Figure 1) was verified under active load in GM's dynamometer lab (Figure 2). Figure 3 shows the inverter efficiency maps in motoring and regeneration.

Figure 1. The next-generation inverter.

The overall design approach was to integrate active components and reduce/eliminate supporting components. The resulting next-generation inverter prototype has integrated the following key features: closed aluminum coolant manifold, power semiconductors and substrates directly attached to the coolant manifold, film capacitor elements built into the coolant manifold frame, press-fit pins for signal and power circuit interconnections, one-piece power semiconductor and bus plane assembly, and gate drive and control circuits on a single printed circuit board.

Figure 2. Then next-generation inverter prototype under active load test in GM's dynamometer laboratory.
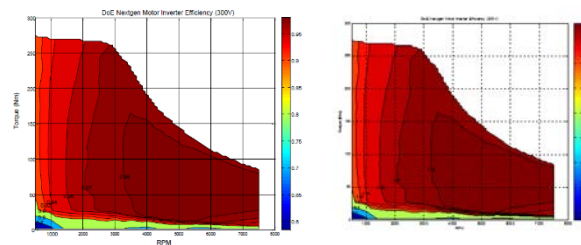
Figure 3. Next-generation inverter efficiency map during regeneration (left) and motoring (right).

Researchers studied key manufacturing processes to ensure the design can be built in high-volume production. Working with GM's internal plant and equipment supplier, a vertically integrated manufacturing plan was developed, which was key in meeting the design and aggressive cost targets.

Ribbon Electrical Interconnects Demonstrate Reliability to Enable Increased Current Density in Power Electronics

Ribbon electrical interconnects of different geometries were subjected to various forms of accelerated testing and exhibited good reliability.

National Renewable Energy Laboratory

The National Renewable Energy Laboratory, collaborating with Kulicke & Soffa, confirmed that ribbon electrical interconnects have good reliability, enabling high-current density power electronics packaging. Transitioning from round wire interconnects to ribbon interconnects affords higher current densities, lower parasitic inductances, and lower loop heights. This transition is key as packages transition to wide bandgap (WBG) devices (Figure 1). A representation of ribbon interconnects at equivalent current density results in a 40% reduction in required bondable area.
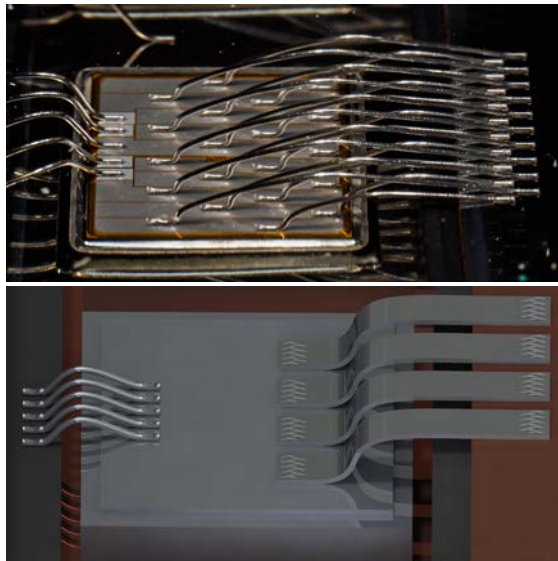
Figure 1. An insulated gate bipolar transistor with wire interconnects from a 2012 Nissan LEAF inverter.

One insulated gate bipolar transistor (IGBT) is rated at approximately 300 amp, and requires twenty 375-μm-diameter aluminum (Al) wires. Four 2,000 μm × 300 μm Al ribbons can replace these wires for a five-fold reduction in needed interconnects. A comparison of the two configurations (Table 1) indicates that ribbon interconnects are a significant enabler for higher-density packaging goals.

	Four 2,000 µm × 300 µm Al ribbons	Twenty 375 µm diameter Al wires
Cross-section (mm^2)	2.4 mm^2	2.2 mm^2
Mutual inductance	++	+
Bonding time(seconds)	2.4	12
Loop heights/heel deformation	++	+
Ultrasonic power/bond force	+	++
Bond pad width (mm)	9 mm	13 mm
Design layout flexibility	+	++
Reliability after accelerated thermal aging, cycling, humidity, and vibration.	Pass	Pass

Table 1. Al ribbon and Al wire at equivalent current densities.

Researchers tested ribbon interconnects of various geometries and materials under elevated temperature (150°C for 1,000 hours), temperature cycling (thermal shock) (-40°C to 150°C, less than 20 seconds transition time), corrosion (121°C, 100% relative humidity for 96 hours), and highly accelerated life test (combined vibration and thermal cycles). The results show ribbon interconnects exhibit similar reliability to wire interconnects under these conditions. Minimizing span length is key to maximizing the lifetime of ribbon interconnects under vibration conditions. This work supports a shift to ribbon interconnects, which enables high-current-density packaging and WBG-based components.

Integrated Wide Bandgap Onboard Charger and DC-DC Converter Shows Double Power Density at Half the Cost

A novel integrated charger architecture and control strategy with wide bandgap devices reduces component count by 47%, direct current bus capacitance by 60%, and losses by 55%.

Oak Ridge National Laboratory

Stand-alone onboard battery chargers (OBC) and 14 volt (V) direct current-direct current (DC-DC) converters that currently dominate plug-in electric vehicles, and all-electric vehicles, are bulky (~0.41 kW/kg, ~0.66 kW/L), not cost effective (~$106/kW), and have relatively low efficiency (85% to 92%) due to limitations of current semiconductor and magnetic materials. This project leapfrogs the present silicon (Si)-based charger technology to address charger and converter cost, weight, volume, and efficiency by overcoming the limitations of Si semiconductor and magnetic materials. It does so by using wide bandgap (WBG) Si carbide (SiC) devices, advanced magnetic materials, and a novel integrated charger architecture and control strategy.

Oak Ridge National Laboratory (ORNL) has developed a new bidirectional integrated OBC and DC-DC converter architecture that reduces the number of components significantly (a 47% reduction in power circuit components alone, not counting savings in the gate driver and control logic circuits, translating to 50% reduction in cost and volume compared to existing standalone OBCs). ORNL has built and tested an all-SiC 6.8 kW bidirectional OBC prototype that integrates a 6.8 kW isolation converter into a 100 kW segmented traction inverter (Figure 1). The isolation converter also has a built-in 2 kW, 14 V buck (voltage reducing) converter to meet vehicle accessory electrical loads.

ORNL has also developed a control strategy for the charger isolation converter to reduce the battery ripple current of twice the alternating current (AC) main frequency that is inherent in single-phase AC-DC converters. Test results show the control strategy reduces the ripple current by 60% and thereby enables a corresponding reduction in the size of the bulky DC link capacitor in the AC-DC front-end converter. Test results also demonstrated high

charging efficiency with a peak value of 96.5% (Table 1) and greater than 55% reduction in losses over a Si-based counterpart.
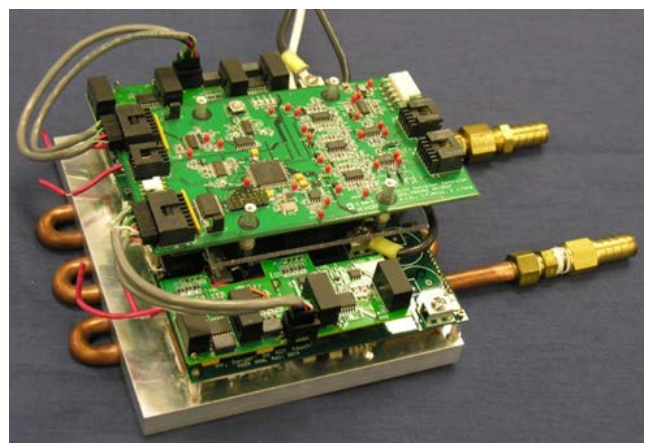
Figure 1. A 6.8 kW SiC charger converter with a built-in 2 kW, 14 V buck converter tested in an integrated SiC bidirectional OBC with a 100 kW segmented traction inverter.

	Power density [kW/L]	Specific Power [kW/kg]	Cost [$/kW]	Efficiency [%]
SOA	~0.66 kW/L	~0.41 kW/kg	~$106	85-92%
ORNL	~1.3 kW/L	~0.8 kW/kg	~$48	93-96.5%

Table 1. Performance comparison against the state-of-the-art (SOA).

Thermal Stack-up Enables Full Potential of Wide Bandgap Devices

Oak Ridge National Laboratory is providing materials science and engineering to support the advancement and maturation of alternative interconnect technologies for next-generation power electronic devices.

Oak Ridge National Laboratory

Materials research and development support is provided to power electronics (PE) research at Oak Ridge National Laboratory (ORNL) via joint funding from the Propulsion Materials and the Electric Drive Technologies programs within the U.S. Department of Energy's Vehicle Technologies Office.

The power module is the heart of PE, and its thermal stack-up is the second most important determining factor in performance second only to the device itself. Thermal stack-up joints are critical in determining reliability and thermal performance. Current state-of-the art interconnects are primarily soldered or brazed (Table 1).

Material	Thermal Conductivity (W/mK)	Forming Temperature °C	Cost per cm² area ($)
Sintered Ag (50% dense)	90 W/mK	250°	$0.08
Tin-Silver-Copper Solder	60 W/mK	185°	$0.01
Braze for Aluminum	67 W/mK	390°	$0.03
Braze for Copper	340 W/mK	750°	$0.02

Table 1. Approximations of thermal conductivity, forming temperature, and cost for contemporary interconnection options.

New sintered-silver (Ag) technology holds promise, but the ability to consistently and effectively create joints utilizing this method is not well understood yet. This project is scientifically examining all of the elements to producing a consistent and reliable sintered joint. Table 2 shows a list of what affects the produced sintered-Ag interconnection. This work has generated quantifiable factors to producing a sintered joint.

Printing method (stencil versus screen).	Topography of the to-be-bonded surfaces.
Print pad thickness, area/size, and shape.	Choice of plating material.
Paste drying method, time, and temperature.	Coefficient of thermal expansion mismatches.
Sintering pressure, temperature, and time.	Sulfidation and oxidation.

Table 2. Some factors examined at ORNL that are observed to affect the quality of sintered-Ag interconnection.

One pathway to hasten sintered-Ag utilization is fundamentally proving its anticipated higher reliability. ORNL developed custom sintered test coupons whose thermal cycling testing is providing needed data for this (Figure 1). ORNL is processing and characterizing the sintered-Ag coupons while the National Renewable Energy Laboratory (NREL) is performing thermal cycling (e.g., -40° to 170°C) to excite failure mechanisms. Failures are correlated to Table 2 factors.
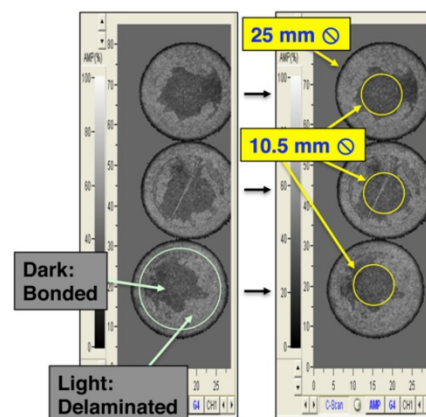

Figure 1. Scanning acoustic microscopy images of delaminated sintered-Ag interconnects. Dark patches represent undelaminated bonding. ORNL and NREL are using such analysis to improve understanding of sintered-Ag reliability.

Electrochemical Energy Storage

High Capacity Solid Electrodes Offer Greater Capacity/Energy Density and Potential Cost Savings

A new type of electrode manufacturing approach promises to both lower electrode cost and enable production of cells with higher energy density.

24M

Lithium-ion battery electrodes have been manufactured using the same basic approach since their introduction approximately 30 years ago. A slurry of active material, binder, and conductive additive is spread onto a current collector, which is then moved through a long drying oven. This process is relatively slow, uses expensive and toxic solvents, and limits the thickness of an electrode to about 150 microns.

24M's novel and inexpensive manufacturing process requires fewer unit operations for higher process yield, and results in electrode and stacked cell fabrication in one-fifth the time and footprint of conventional stacked cell lines. The semisolid electrodes developed by 24M require no drying and no organic solvents. In addition, the process is able to make thick electrodes, from 200-1,000 microns. This increases the energy density and has the potential to reduce the cost of stacked cells due to a decreased amount of "non-energy storing" materials in each cell, such as a separator and current collector.

Historically, attempts at making thicker electrodes have faced two issues. The first is that the current process can only dry electrodes up to about 150 microns. Thicker electrodes either crack at the top layer, or do not dry completely near the bottom. The second is that thick electrodes often suffer from poor power. 24M's electrodes show both excellent energy and power capability (Figure 1). The enhanced areal capacity of 24M's electrodes, the amount of capacity (or energy) they store per unit area of the electrode, is two to four times that of conventional electrodes. At higher rates (or higher current densities), the 24M electrodes still outperform conventional electrodes.

As part of their current development program, 24M increased cathode and anode volume loadings to greater than 50 volume percentage; scaled up and improved manufacturing, achieving greater than 90% electrode yield with weight and thickness tolerances of less than ±5% for both cathode and anode electrodes; achieved 89% and 90% cell yield for cathodes and anodes based on capacity and impedance tolerances of ±5% and ±10%, respectively; and delivered 10 cells (of 4.5Ah capacity) to Argonne National Laboratory for testing.
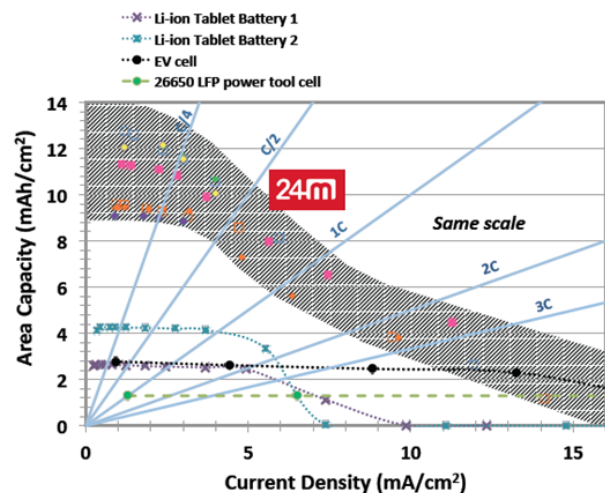
Figure 1. Comparative capacity per unit area of cells using 24M electrodes (shaded area) versus traditional cells (curves shown near 2 and 4 mAh/cm²), both plotted as a function of current density, or cell discharge power. The 24M cells range in capacity from .003Ah to 2Ahr.

National Laboratory Teams with Strem Chemicals to Provide Next-Generation Energy Storage Materials

Nine battery electrolyte materials invented at Argonne National Laboratory will be produced, marketed, and distributed by Strem, a manufacturer and distributor of specialty chemicals.

Argonne National Laboratory

Argonne National Laboratory (ANL) has teamed with Strem Chemicals, Inc., to provide industry and the battery research community with next-generation energy storage materials.

ANL's Materials Engineering Research Facility (MERF) supports the laboratory's Advanced Battery Materials Synthesis and Manufacturing R&D Program by providing scale-up support for promising battery materials. The MERF is enabling the development of manufacturing processes for producing advanced battery materials in sufficient quantity for industrial testing. By bridging the gap between small-scale laboratory research and high-volume battery manufacturing, research at the MERF will support progress in the development, validation and ultimate commercialization of advanced battery materials chemistries.

Specifically, Strem, a manufacturer and distributor of specialty chemicals founded in 1964, has licensed 23 separate pieces of intellectual property from ANL and will distribute nine battery solvents and additives via its marketing and global distribution networks. ANL invented these electrolyte materials and initially scaled up at MERF. Three of those materials are shown in Figure 1. "We continue to receive requests for samples of materials that we have scaled but have fully distributed," said MERF director Greg Krumdick. "Partnering with Strem made sense to help make these materials available."

MERF will provide guidance on the synthesis and validation to ensure that the materials produced meet the required chemical purity and electrochemical performance prior to distribution. "This agreement helps us get these materials out the door and into the hands of industry and researchers," said Krumdick. "It takes us one step

closer to our final goal, implementation in commercial batteries."

The agreement with Strem both funds and exemplifies successful technology transfer across the research spectrum: from invention at the bench to scale-up, and ultimately into use by industry.

Figure 1. Three of nine electrolyte materials licensed to STREM from ANL for marketing, sales, and distribution.

Statistical Verification in Small-Scale R&D

In benchtop lithium-ion research, insufficient process standards and statistical verification of data may result in conflicting information and hinder progress. Researchers have de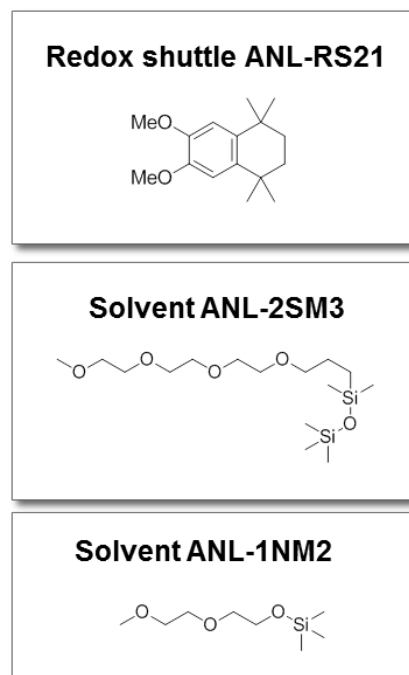veloped and are implementing more standard procedures, including statistical verification, to enable more efficient materials discovery.

Argonne National Laboratory

Small-format cells, such as the 2032-type coin-cell, offer a fast and convenient way to screen the electrochemical properties of lithium-ion materials. Therefore, the coin-cell is used prolifically in small-scale research and development. However, within some organizations, there has been insufficient attention to the degree of process control inherent to this type of hand-assembled cell. Consequently, conflicting or misleading data, unrelated to actual materials properties, can result and hinder efficient progress in discovery and understanding.

Researchers at Argonne National Laboratory (ANL) are advancing standardized protocols and procedures related to full-cell and coin-cell construction, electrochemical testing, and data analysis. Coin-cell testing results in "performance bands" for a given metric (e.g., capacity, impedance, and energy) and these bands can span a significant range of values (Figure 1, top). In addition, when dealing with new chemistries, identifying and eliminating outliers is not always justified. To minimize the inherent variability of this cell format, the ANL team has characterized baseline chemistries using 30-cell sets and standard protocols. A bootstrap analysis, or resampling, of the data can be done with any metric of interest. Bootstrapping creates distributions at every sample size N along with the associated confidence limits. A continuous "probability (P) map" as a function of sample size is assembled from those distributions (Figure 1, bottom). Once this analysis is complete, new chemistries can be tested at smaller sample sizes.

For example, a modification to the baseline was incorporated into N=5 cells. The 30-cell baseline set permitted this N=5 sample size to be analyzed with statistical confidence. The modified set (red circle) showed slightly lower average impedance rise compared to the baseline but the improvement is not statistically significant. These protocols will greatly improve the efficiency of materials discovery and better inform resource allocations for scale-up and large-format testing of new materials.
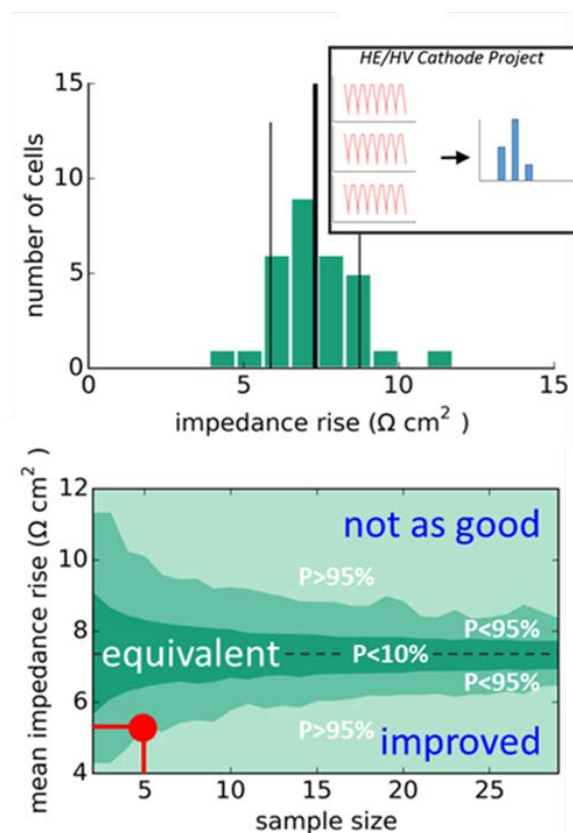

Figure 1. Top graph portrays "Performance band" illustrated as a histogram for the impedance rise of 30 identical, cycled NCA/graphite coin-cells. Inset shows the interface of custom analysis software developed at ANL. Bottom graph exhibits bootstrap "probability map" analysis of the baseline set. Red dot shows a modified 5-cell set against the baseline map.

Probing Conductivity of Battery Electrodes

A new type of probe enables manufacturers and researchers to reliably determine the conductivity of thin-film electrodes, providing information that can improve battery design and performance.

Brigham Young University

One obstacle to large-format battery manufacturing is ensuring uniformity in the manufacturing process. Ensuring uniformity can help make certain that all components perform equally well and no component contributes unduly to performance limitations.

Researchers at Brigham Young University are seeking to improve understanding of material heterogeneities in thin-film electrodes for lithium-ion batteries, and how those variations lead to performance problems. Researchers developed a new surface probe that can accurately measure conductive properties of intact battery electrodes. Measuring conductivity of thin-film electrodes (still attached to the metallic current collector) is difficult, and prior methods have not been sufficiently reproducible as the current collector impacts the measurement. The new method overcomes these problems and allows simultaneous measurement of two critical properties: bulk film conductivity and contact resistance between the film and the current collector. The probe is fabricated using semiconductor clean-room techniques. Researchers use a computer model to interpret the experimental results. A computer-controlled fixture allows the probe to be scanned across the electrode surface, creating a conductivity map. In effect, "hot" and "cold" conductivity spots can be identified so that electrode process quality can be improved.

One surprising observation was the large degree of conductivity variability, on a millimeter length scale, of commercial-grade electrodes (Figure 1). This result likely means that the electrode must be "overdesigned" to account for poor performance in some regions of the electrode. Overdesigning for conductivity means that other desirable properties, such as energy density, are sacrificed.

The probe has been validated using existing methods with several commercially produced electrodes, on delaminated electrodes, and on conductive silicone. Prototypes have been delivered to A123 for its use in quality control. The technology is likewise available for licensing by other manufacturers.
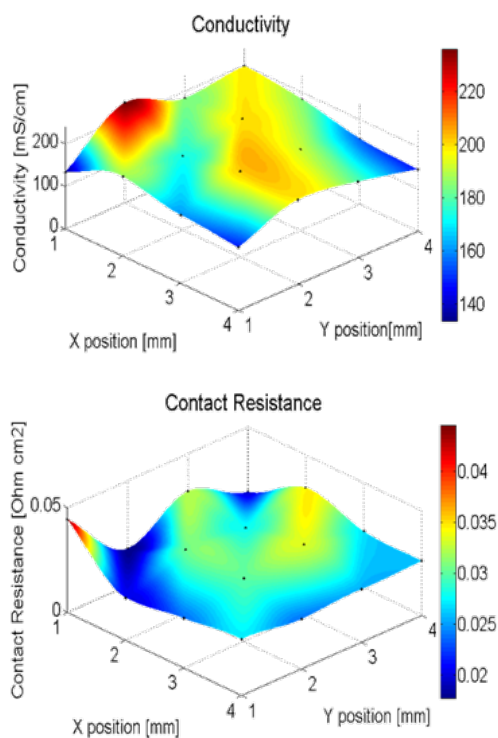

Figure 1. Measured bulk conductivity and contact resistance as functions of position for a Toda 523 cathode on aluminum current collector (material provided by Argonne National Laboratory).

Reduced-Cost Lithium-Ion Cells via Improved Manufacturing Processes

A number of cost reduction approaches, including fast formation, non-NMP coating, and direct separator coating, resulted in cells with similar performance and a 50% manufacturing cost reduction.

Johnson Controls, Inc.

The objective of this effort was to employ a portfolio of advanced manufacturing technologies to demonstrate a 50% manufacturing cost reduction in large-format lithium-ion cells. Three key opportunities in cell manufacture were targeted: a faster cell formation process, an electrode made using a non-N-Methylpyrrolidone (NMP) based process, and a direct separator coating. Integrating these three advanced manufacturing technologies achieved the targeted cost savings by eliminating material, lowering capital equipment expenditures, and reducing energy and manufacturing costs. This project also demonstrated reductions in the environmental impact of battery production through the concomitant reduction in greenhouse gas emissions and eliminating solvents.

The following summarizes the goal sought for each area of focus:

- Dry (non-NMP) electrode: Improve electrode micro-structure and morphology and develop the process for an automated pilot line for large-format cell builds.
- Aqueous (non-NMP) cathode: Develop an additive and new formulation for mixing and coating process improvements.
- Direct coated separator: Develop a roll-to-roll process for scale-up to improve lamination strength and reduce thickness variation.
- Fast Formation: Develop a new activation process to improve cell uniformity using step-charging and step-aging processes and develop an improved internal short detection process at low states of charges.

The key accomplishments in these areas include the following:

- Dry electrode: Cells built with the final version of the dry electrode process demonstrated comparable performance to the baseline cells (Figure 1) with a 53% cost reduction versus the wet coating process.
- Aqueous cathode cells: Cells employing aqueous cathode cells demonstrated 98% of the performance of the baseline design and a 3.5% cost reduction compared to the NMP-based electrode process. The cells with the newly developed mixing process delivered promising performance and quality as well.
- Direct coated separator cells: Cells employing direct coated separate cells demonstrated 27% better rate capability compared to the baseline and a 56% cost reduction in the assembly process compared to the conventional polyethylene separator.
- Fast Formation: This activation process reduced formation time from 24 to 7 days with excellent performance and internal short detectability.
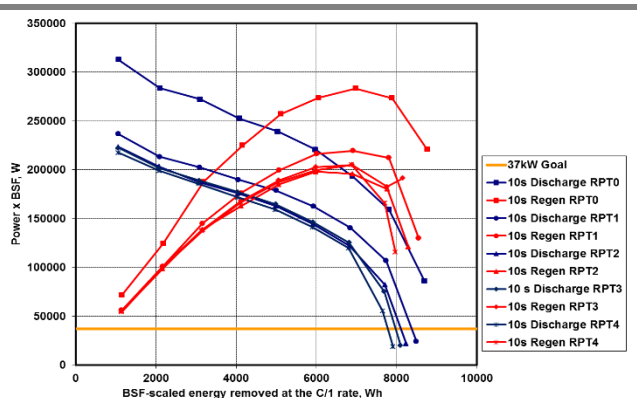
Figure 1. Cycle life data (~1,000 cycles) at 30°C of a cell with dry processed anode and cathode electrodes. The dry processed cell is showing fade rates consistent with a cell using traditionally processed electrodes.

Rapid, Low-Cost Battery Electrode Dryer

A small footprint, variable frequency microwave drying technology uses less energy than conventional electrode ovens and results in more rapid drying.

Lambda Technologies and Navitas Systems

High battery cost is a key factor limiting the adoption of electric vehicles. In high-volume production of electrodes for lithium-ion batteries, electrode drying is the largest operational unit cost. In conventional processes, electrode slurries are cast onto metal foils and dried under highly controlled conditions in very long ovens. The oven length is dictated by the limited rate at which the electrode can be completely dried to meet quality and performance specifications.

Lambda Technologies and Navitas Systems' innovative variable frequency microwave (VFM) drying technology employs penetrating energy that selectively targets the solvent in the entire volume of the wet electrode, which simultaneously drives out the solvent. High-frequency infrared (IR) or convection dryers heat only the surface (Figure 1), and solvent removal in proceeds layer by layer as heat transfers inwards; this drying process takes longer than VFM (Figure 2). VFM results in an estimated a 30% to 50% reduction in the operating cost of electrode drying.

All electrode material properties and performance characteristics are identical for cells produced using VFM or conventional drying methods. The cycle life testing for cells produced by both methods are shown in Figure 3; the performance is identical, demonstrating the technical feasibility of a small footprint, low-energy, and rapid drying process.

The newly assembled VFM roll-to-roll dryer is now installed at a battery manufacturer for pilot line production, with results to be reported next year. Battery manufacturers and production line integration companies have expressed interest in adopting VFM ovens into production.

Figure 1. Comparison of innovative VFM drying process, with high-frequency IR heating and convection surface heating methods. Heat energy distribution shown in red.

Figure 2. Drying time comparison between conventional and VFM dryer.
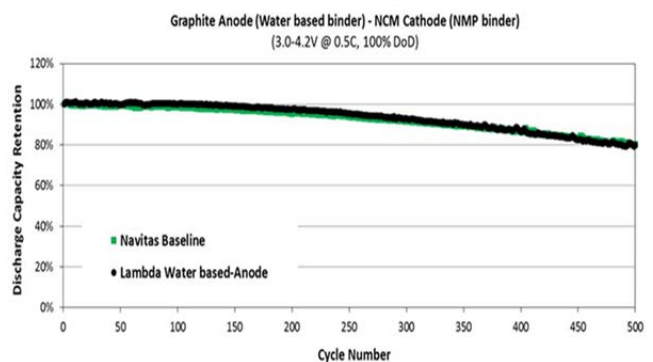
Figure 3. Cycle life testing for battery cells show identical performance of battery electrodes dried with VFM (Lambda).

Understanding Cathode-Anode Degradation in Lithium-Ion Batteries

Work provides critical understanding of an important degradation mechanism in high-energy density lithium-ion cells for electric vehicles.
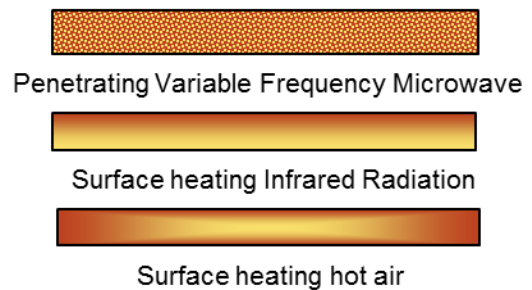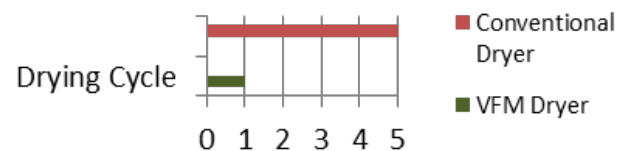
Lawrence Berkeley National Laboratory

Rechargeable lithium (Li)-ion batteries continue to be at the forefront of energy storage technology with their dominance of the portable electronics market and incipient penetration in large-scale applications, such as electric vehicles. However, existing battery performance limitations, which originate from slow transport and irreversible changes in the battery cell during long-term operation, inhibit widespread deployment of Li-ion batteries in the transportation sector. Degradation is shown to be due to formation of unique nickel (Ni) and manganese (Mn) coordination complexes, which contribute to power and capacity loss.

The Li-ion battery is an example of an inherently unstable electrical energy storage system. For instance, electrochemical oxidation of the electrolyte at the cathode results in surface film formation, which helps extend battery life. However, the electrolyte oxidation is accompanied by dissolution of trace amounts of transition metals (such as Ni, Mn, and cobalt), which penetrate into the electrolyte and cause loss of electrochemical performance of the graphite anode and the entire Li-ion cell.

Researchers used a variety of advanced analytical methods to demonstrate that electrochemical oxidation of the electrolyte at a model Li-ion positive electrode leads to the formation of unique fluorescent Ni and Mn coordination complexes, which dissolve into the electrolyte and are ultimately incorporated into the surface layer on the graphite negative electrode. The Mn and Ni complexes incorporated into the anode inhibits Li-ion transport and contribute to battery cell impedance rise and capacity loss (Figure 1).

This work displays the mechanism of transition metal dissolution and anode "poisoning," and reveals a unique insight into the mechanism of Li+

transport kinetics in Li-ion. The research demonstrates that such a chemical cross-talk between electrodes may universally occur in all high-energy Li-ion cells based on transition-metal oxide positive electrodes and organic-carbonate-based electrolytes.

This study helps resolve uncertainties about the origins of this detrimental "poisoning" effect in Li-ion batteries, and supports the more informed design of effective counter measures to electrodes and materials instability in Li-ion batteries for transportation applications.

Figure 1. Effect of Mn and Ni poisoning on the Li-ion cell impedance (top). Molecular mechanism of electrolyte oxidation and Ni and Mn coordination complexes formation (bottom).

Underhood Lithium Stop/Start Battery Prototyped
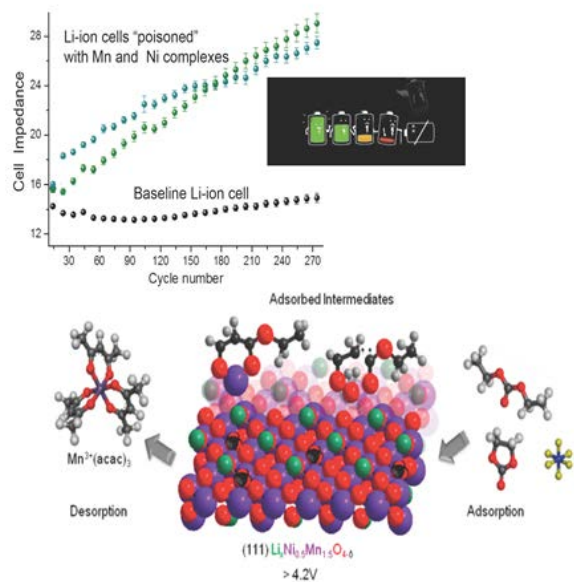
Drop-in replacement for existing car battery minimizes integration requirements while providing the fuel economy benefits of stop/start technology.

LG Chem Power Inc. with the U.S. Advanced Battery Consortium

Stop/start technology has been demonstrated to provide improved fuel economy and reduced idling emissions. Typically, a second battery is required; it is generally placed in the trunk or similar location to protect the battery from degradation caused by the extreme heat of the engine compartment. Using two batteries in separate locations adds cost and complexity. Preferably, the benefits of stop/start technology would be delivered by a single battery that could survive in the engine compartment, a location used today for the starter battery.

LG Chem Power Inc. (LG-CPI) has developed a prototype design based on resilient lithium (Li) titanium oxide–Li manganese oxide (LTO-LMO) cells and an insulated case. The LTO-LMO chemistry recharges well due to the geometry of the material at the molecular level. The ability to accept charge rapidly, even at low temperatures, potentially makes these electrodes efficient at capturing the energy normally lost in braking. Another benefit is that LTO-LMO batteries are typically less prone to problems in abuse testing.

However, there have been challenges with using LTO-LMO batteries in the past. Even though the LTO electrode can accept Li ions at low temperature, typical electrolytes can slow the process down and reduce the ability to accept energy from braking at very cold temperatures, such as -30°C. The relatively low voltage of a single LTO-LMO battery cell makes it hard to store sufficient energy inexpensively. Finally, they can experience degradation at higher temperatures. This makes implementation in the engine compartment, where temperatures can exceed 100°C, a serious challenge.

LG-CPI has addressed each of these problems. Advanced cell design and material improvements have reduced the impact of low temperature; while

additives, manufacturing technique, and a unique insulated pack design taken together help the batteries survive in the under-hood location typically occupied by the heavier and less efficient lead acid battery used in vehicles today. In Figure 1, the cells are predicted to stay at a very acceptable temperature of 50°C even after four hours of exposure to fairly common engine compartment operating temperatures. The first-generation cells are about to undergo testing to determine if they meet the U.S. Advanced Battery Consortium goals.
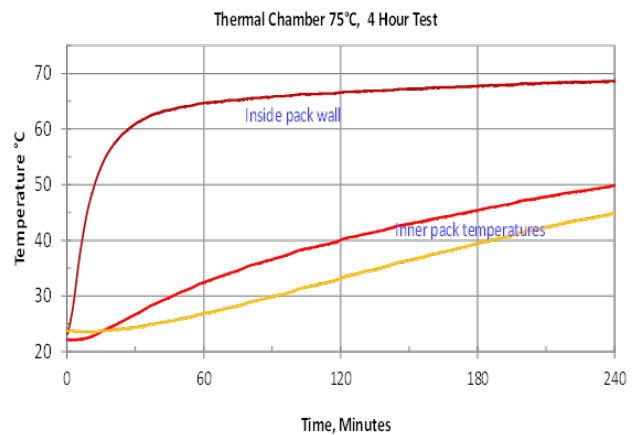
Figure 1. Combining the thermal inertia of the cells with the unique insulated design, LG-CPI predicts the LTO-LMO cells will stay below 50°C for four hours when the pack is exposed to 75°C ambient temperature, which is common where an operating engine is housed in a vehicle.

Magnetic Field Manufacturing of High-Energy Electrodes

Advanced route to thicker electrodes and higher energy electric vehicle batteries demonstrated.

Massachusetts Institute of Technology

The lithium (Li)-ion battery, now 25 years old, is indisputably a highly successful technology. In order to meet electric vehicle technology goals, however, some inherent limitations must be overcome. One longstanding Li-ion limitation has been long and tortuous Li-ion transport paths through the electrodes. These long paths are a natural consequence of the high-pressure compaction typically used in manufacturing Li-ion electrodes. The high electrode tortuosity normal to the electrode plane causes a cascade of inefficiencies in battery design; the battery electrodes must be thin enough to provide the power needed for vehicles, which increases the relative amount of non-energy-storing components, resulting in the energy density and cost/kWh of the batteries to suffer. Practical methods are needed for achieving reduced tortuosity (line-of-sight) pore channels oriented to the electrode plane.

In this project, researchers used magnetic fields to quickly and efficiently produce more ideal Li-ion pathways from sacrificial pore-formers. A small amount of magnetic nanoparticle fluid is dispersed on nylon rods as part of the emulsion within the battery electrode suspension while it is still fluid. Each droplet is a micro-magnet, and under an imposed magnetic field, lines up the nylon rods with each of its neighbors forming chains aligned with the applied field. The chains in turn repel one another, forming a periodic array. Removing the chained droplets leaves a more ideally oriented porosity. Figure 1 shows results for a typical (lithium cobalt oxide ($LiCoO_2$)) cathode, sintered for consolidation after magnetic alignment and removal of the sacrificial pore-former.

This magnetically processed and aligned electrode delivers more than twice the areal capacity as the same electrode in the absence of alignment. At 8.1

mAh/cm^2, this electrode also has more than twice the areal capacity of current cells, which may drive down the cell's cost due to the reduction in non-energy-storing components such as separators and current collectors.

With further development, the magnetically-assisted porosity engineering approach could find use in existing electrode manufacturing processes or be incorporated into new battery manufacturing methods.
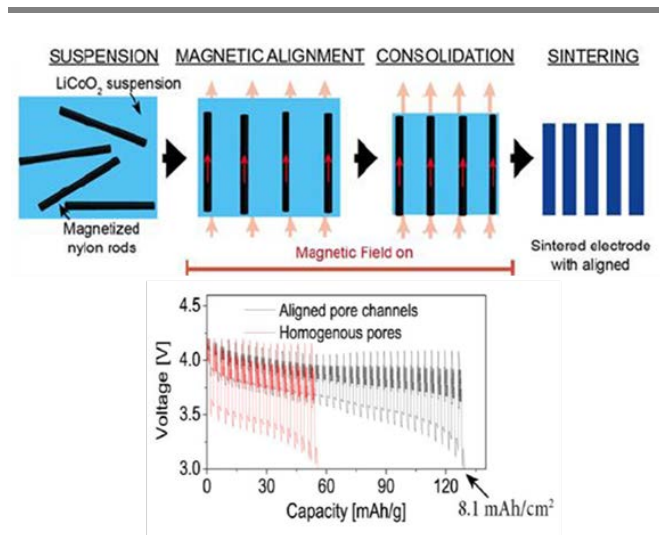
Figure 1. Magnetic alignment of emulsion droplets produces oriented, uniformly spaced, low-tortuosity, porosity oriented normal to the electrode plane (top). Dynamic stress test cycling of cells with aligned and non-aligned (homogeneous) electrodes with loadings three-times higher than standard electrodes (8.1 vs. ~3 mAh/cm^2) (bottom).

Supercapacitors Matched with Batteries Reap Advantages of Both

Power intensive supercapacitors and energy intensive batteries make for an improved stop/start system.

Maxwell Technologies, Inc. with the U.S. Advanced Battery Consortium

Engine stop/start technology has been demonstrated to improve fuel economy and reduce idling emissions. Combining the needed power and energy in a single and more efficient package to support this technology, however, has been subject to limitations. Typically, a second battery is required, often placed in the trunk or a similar location to protect the battery from degradation caused by the extreme heat it would experience if it were located in the engine compartment. Recently, supercapacitors have been used as the second power source. Supercapacitors deliver or accept power very rapidly and some supercapacitors suffer very little loss of performance at low temperature, offering unique capabilities for a 12 volt (V) stop/start system.

Maxwell has developed a single unit 12 V package that combines advanced lithium (Li) iron phosphate battery cells with 3,000 farad (F) supercapacitors. This unique design takes advantage of the power of supercapacitors and the energy storage capability of Li-ion batteries. In cold or high-power situations, the supercapacitors deliver almost all the power, while the battery cells provide power in longer but lower power events, and recharge the supercapacitors if a retry at starting is required.

Researchers built a "mule" system that is ready for testing to prove the concept. Using two parallel strings of four advanced A123 cells, which have good performance at -30°C, wired in direct parallel with six 3,000F Maxwell supercapacitors, the challenging U.S. Advanced Battery Consortium cold start goal can be met with significant extra capacity. These results are highlighted in Figure 1, where the voltage maintains a value greater than the minimum allowed, 8 V, during the three, cold crank pulses. By using a parallel configuration, much of the monitoring and balancing hardware can be eliminated, taking advantage of the safety record of these two types of cells to lower part count and the need for expensive voltage convertors.

In an effort to further reduce system volume, mass, and cost, researchers initiated a second task that involves developing a pouch supercapacitor. The team is making significant progress in reducing gas formation at the voltages and temperatures anticipated in an out-of-the-engine compartment implementation. If successful, this could also positively impact other supercapacitor applications, beyond automotive.
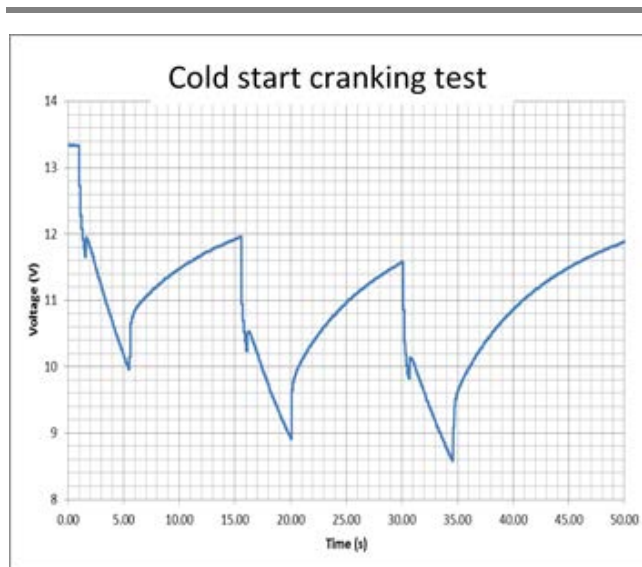

Figure 1. The voltage and current of the 12 V stop/start system stays well above the requirement for all engine "cranking" events in the -30°C cold start test. This leaves room for acceptable performance after degradation over the life of the system.

High-Speed, High-Fidelity Battery Model Development

The successful development of a fast-running, high-resolution battery model will encourage using computer models for electric-drive vehicle battery system design and evaluation, potentially allowing for more rapid development cycles and lower costs in the battery development process.

National Renewable Energy Laboratory

In support of the U.S. Department of Energy's Computer Aided Engineering for Electric-Drive Vehicle Batteries (CAEBAT) project, the National Renewable Energy Laboratory (NREL) pioneered the multiscale multi-domain (MSMD) model, overcoming challenges in modeling the highly nonlinear multi-scale response of battery systems. The MSMD model provides significant flexibility and multi-physics expandability through its modularized architecture, as well as computational efficiency. The original MSMD model was validated against experimental cell data by the CAEBAT team, including Ansys, General Motors, and NREL, and has been integrated into the Ansys program. However, a further increase in computational speed was needed to promote the application of the multi-physics model to battery engineering problems. Recently, NREL developed a new quasi-explicit nonlinear multiscale model framework, the GH-MSMD, using time-scale separation, variable decomposition, and partial linearization that increased computational speed by a factor of over 1,000. The GH-MSMD approach eliminates several layers of nested iteration, significantly improves model speed and stability, and retains the modular framework architecture that is critical for battery behavior simulations.

In fiscal year (FY) 2014, NREL met the 100-fold computational speed-enhancement target for its multiscale multi-physics battery model one year ahead of schedule. In FY 2015, NREL exceeded the target by improving the code structure and extending the model to a larger scale.

Figure 1 presents the comparison of the electrical and thermal response of a battery for a mid-size sedan plug-in hybrid electric vehicle (PHEV10) on the U.S. Environmental Protection Agency's Highway (US-06) 20-minute driving profile, and also the time for simulations to be completed using the original, enhanced, and latest simulations. While the two models yield essentially identical results, at commercially relevant and identical discretization levels, the GH-MSMD approach demonstrates that the most efficient electrode-domain model option can run a 1,200-second driving profile simulation in 0.74 seconds using a personal computer. This is approximately 1,000-times faster than the original MSMD model that runs the same profile in 654 seconds. This approach achieves significant speed-up while maintaining model fidelity. Current and future efforts are focused on expanding the applicability of the new model to a wider variety of battery engineering problems.
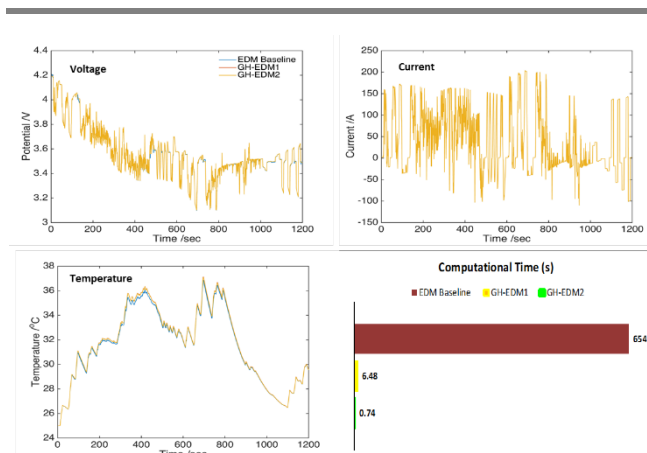
Figure 1. Comparison of electrical and thermal response of a battery for a mid-size sedan PHEV10 on the US-06 20-minute driving profile from the GH-MSMD and the original MSMD. Bottom right image shows the time to simulate the driving profile using the three simulations.

Internal Short-Circuit Device for Battery Abuse Testing

Device passively triggers internal short circuits to afford more realistic evaluation of abuse tolerance impacts of cell materials and design choices.

National Renewable Energy Laboratory

While the energy and power densities of lithium (Li)-ion batteries make them the current industry choice for plug-in electric vehicles, thermal safety of these batteries must be considered as vehicle battery system designs are evaluated. Internal short circuits (ISCs) triggered by minor latent internal flaws can lead to thermal runaway. It is believed that ISCs, coupled with a lack of mitigation technology at the system level, caused battery failures in the Boeing 787, which resulted in the new airplane's grounding and a $500 million loss for the companies involved.

Until now, most methods for inducing an ISC – nail penetration, rod penetration, crushing, applying voltage, or significantly increasing temperature beyond normal ranges – have tampered with the cell exterior, and do not permit the short to be precisely positioned within the cell. The National Renewable Energy Laboratory's (NREL) recently-patented ISC device provides a precise, highly repeatable way to create a true internal short, evaluate and predict reactions, and use in the design of battery cells and packs. The thin, easy-to-implant device is capable of emulating ISCs and latent defects, delivering consistent and controllable short circuits. It can be used in a wide array of cell configurations and chemistries to reliably produce all four types of shorts – electrode to electrode, electrode to cathode, electrode to anode, and cathode to anode – each of which illicit responses from benign to severe.

The simple device has no moving parts and is composed of a small copper and aluminum disc, a copper puck, a polyethylene or polypropylene separator, and a thin layer of wax (Figure 1). After device implantation, an ISC is induced by raising the cell temperature to 40°C to 60°C to melt the wax layer, which is then wicked away by the separator, putting positive and negative sides in contact and inducing an internal short (Figure 2).

After several design iterations, NREL has delivered more than 300 ISC devices to the National Aeronautics and Space Administration and several industry partners for use in evaluating the abuse tolerance of new cell designs and materials, as well as cell-to-cell propagation in modules. Conversations to produce the ISC device on higher volume with automation are underway with manufacturers. NREL can provide samples of the ISC device to interested parties for evaluation of the abuse tolerance performance of cells and modules.
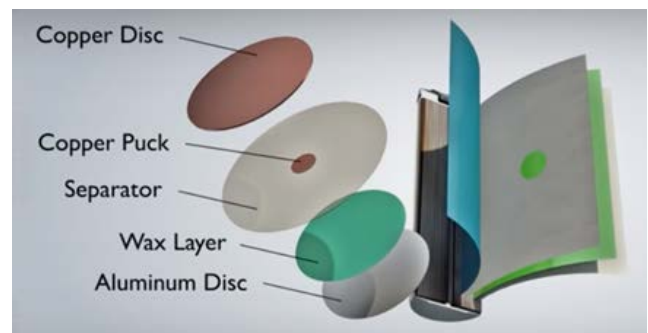

Figure 1. Components of ISC device that can be placed anywhere in a cylindrical or prismatic cell.

Figure 2. Left to right: A Li-ion cell with ISC device, a few minutes after melting the wax, and going into thermal runaway.

Novel Electrolyte Enables Wide Temperature Operation

An electrolyte for lithium-ion batteries improves both low-temperature power and high-temperature life, two important features in both electric vehicle and stop/start batteries.

Pacific Northwest National Laboratory

The battery research team at Pacific Northwest National Laboratory (PNNL) has successfully developed novel non-aqueous electrolytes for lithium-ion batteries (LIBs) to operate over a temperature range of –40°C to +60°C with improved low-temperature capacity and high-temperature capacity retention. These electrolytes will enable greater functionality in electric vehicles operated in extreme weather conditions, as well as in stop/start operation applications at low temperatures.

State-of-the-art LIBs using conventional electrolytes can operate well in the temperature window of -20°C to +40°C, but the power of these batteries drops quickly at lower temperatures. The lifetime of the batteries also degrades quickly when operated at temperatures above +45°C. Although some electrolytes enable good battery performance either at low temperatures (down to –40°C) or at high temperatures (up to +55°C), most of these electrolytes cannot work well over life at both high and low temperatures.

The PNNL team has developed novel salt additives for electrolytes used in LIBs. Such salt additives (at less than 1.5% by weight in the electrolytes) allow the use of propylene carbonate, a beneficial solvent for low-temperature application and cost reduction. The salt additives also lead to the formation of an ultrathin, uniform, compact and robust protection layer (solid electrolyte interphase (SEI)) on the surface of the graphite anode. This SEI layer is critical for the stable operation of LIBs. This layer maintains its thickness during the long-term operation of the LIBs even at high (+60°C) and very low (–40°C) temperatures. It also reduces the battery's internal resistance, thus increasing the rate capability and low-temperature discharge performance. Figure 1A shows that LIBs using

PNNL's new electrolyte maintain 81% of their full capacity after 100 cycles at +60°C, while the LIBs with a typical conventional electrolyte can retain only 61% of the initial capacity. Figure 1B shows that LIBs using PNNL's new electrolyte can retain 61% of their full capacity at –40°C, which is much more than with the conventional electrolyte where only 18% of the room temperature capacity is retained. Therefore, PNNL's novel electrolytes can significantly broaden the operational temperature window of LIBs used in electric vehicles, especially for low-temperature operation. These electrolytes can also enable LIBs to be used as the power supply for stop/start operation of vehicles used in extreme weather conditions.
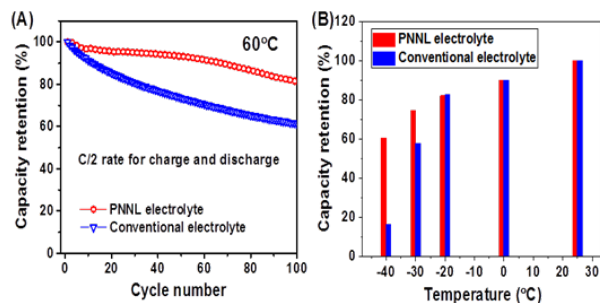
Figure 1. Discharge capacity retention of graphite, aluminum-doped lithium nickel oxide full cells with cycling at +60°C (A) and at ambient and low temperatures (B). The batteries using PNNL electrolyte shows significantly improved capacity retention at both high (+60°C) and low (–40°C) temperatures.

Solid-State Module Technology Demonstrated

Lithium-metal chemistry shows promise for next-generation electric vehicles.

Seeo Inc. with U.S. Advanced Battery Consortium

Seeo Inc. has developed an all-solid-state battery technology that utilizes lightweight lithium-metal anodes and is enabled by Seeo's proprietary DryLyte™ polymer separator technology. The present Seeo cell is designed to operate at elevated temperatures (70° to 90°C). Seeo developed a module technology to perform automatic temperature control and interface with electric vehicle powertrains. Each of the early demonstrator modules provided to the U.S. Advanced Battery Consortium (USABC) contain 48 cells in series (Figure 1), and each is nominally rated at 11Ah, 1,800Wh, and 140Wh/kg. This technology has fundamental potential to reach 400Wh/kg (cell), which is 50% higher than incumbent technologies.

Seeo built six modules and thermal management test fixtures, and provided three to the USABC for electrical testing at Argonne National Laboratory, thermal testing at the National Renewable Energy Laboratory, and abuse testing at Sandia National Laboratories. Three modules were tested separately at Seeo. USABC developed test plans to evaluate the modules against automotive standards.

Testing highlights include average module-level results taken at 80°C internal in 30°C ambient environments. Discharge tests yielded 1,807Wh (144Wh/kg) with C/3 discharges, and stable discharge behavior after 200 cycles of dynamic stress testing at 225W/kg (Figure 2). Power evaluation tests yielded 241W/kg and 258W/L peak power ratings (at 80% depth-of-discharge), and successful discharges were achieved with the U.S. Environmental Protection Agency's highway profile at 438W/kg (module-level, to 80% depth-of-discharge). Safety testing showed successful completion of a thermal ramp abuse test to 150°C without venting or thermal runaway.

Remaining challenges for the technology include decreased power performance at typical low temperatures. In August 2015, Robert Bosch LLC acquired Seeo as a wholly-owned subsidiary. Continued R&D efforts will address this issue and others as Robert Bosch plans to commercialize this technology for use in low-cost electric vehicle battery packs having double the specific energy of the technology demonstrated here, while retaining all of the required safety aspects.
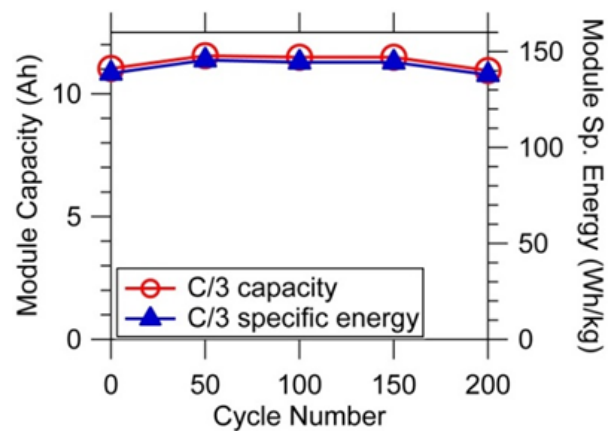

Figure 1. Seeo 11Ah cell and 1,800Wh module.

Figure 2. Performance tests (80°C) show stable discharge capacity after 200 DST225 cycles.

Core-Shell Nanoparticles Improve Performance

Li_xSi-Li_2O nanoparticles can be mixed with various anode materials to improve 1st cycle Coulombic efficiency and cell energy.

Stanford University

Lithium (Li)-ion batteries are widely used for consumer electronics and exhibit great potential for electric vehicles and grid-scale energy storage. Rapid progress has been made in realizing battery electrode materials with high capacity and long-term cyclability in the past decade. However, low 1st cycle Coulombic efficiency (CE) as a result of forming solid electrolyte interphase layers remains unresolved, especially for high-energy anode materials such as silicon (Si) and tin, which offer up to 10 times the capacity of standard carbon. As a result, the cell's overall energy density is reduced as the irreversible capacity in the anode is compensated by increasing the loading of the cathode.

Stanford University has developed Li_xSi-Li_2O core-shell nanoparticles (NPs) as a high-capacity prelithiation reagent to compensate the 1st cycle irreversible capacity loss of various anode materials, such as graphite and Si. Researchers synthesized Li_xSi NPs by mechanically stirring a mixture of Si NPs and Li metal at elevated temperature under an argon atmosphere. A dense passivation layer is formed on the Li_xSi NPs after exposure to trace amounts of oxygen (O), preventing the Li_xSi from further oxidation in dry air (Figure 1a). Scanning transmission electron microscopy (STEM) shows a dense passivation layer of Li_2O on the surface of the Li_xSi NPs (Figure 1b). The unique core-shell structure gives the prelithiation reagents excellent stability in dry air, indicating that these NPs are potentially compatible with industrial battery fabrication processes.

Li_xSi-Li_2O core-shell NPs can be mixed with various anode materials during slurry processing to improve the 1st cycle CE. The prelithiation capacity of Li_xSi-Li_2O NPs is 1,000 mAh/g, based on the mass of composite. First cycle voltage profiles of Si NPs/Li_xSi-Li_2O composite and Si NPs show that

incorporating this prelithiation reagent compensates the capacity loss of Si NPs (Figure 1c, capacity is given in grams of Si). The composite (red curve) shows an initial loss of only 10%, whereas the Si NPs (blue curve) show an initial loss of 30%. As mentioned previously, in full cells, that initial loss of Li must be provided by excess cathode, which effectively reduces the energy of the cell.
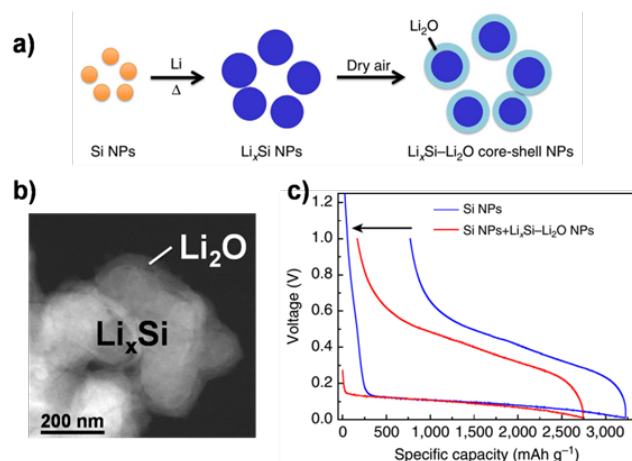
Figure 1. (a) Schematic representation of Li_xSi-Li_2O NPs synthesis method. (b) STEM image of Li_xSi-Li_2O NPs. (c) 1st cycle voltage profiles of Si NPs/Li_xSi-Li_2O and Si NPs show that incorporating Li_xSi-Li_2O NPs compensates the 1st cycle capacity loss of Si NPs.

Fuel Cells

Platinum Monolayer Electrocatalysts on Low-Cost Cores

New catalysts developed by depositing a single layer of platinum atoms on a highly stable, low-cost core with a precious group metal interlayer show roughly three times higher activity than state of the art platinum catalysts.

Brookhaven National Laboratory

A most significant obstacle to the large-scale commercialization of fuel cell vehicles is the high-cost of the fuel cell system. Platinum catalysts account for nearly 20% of the overall system cost at high volumes. By increasing the activity and the stability of the platinum catalyst, the amount of platinum used can be reduced and correspondingly the cost of the fuel cell system.

Brookhaven National Laboratory (BNL) has developed a suite of synthesis techniques to optimize catalyst mass activity and stability. One such approach employs a low-cost core with a palladium shell and a monolayer of platinum as the outer surface. Figure 1 shows a high-resolution image where palladium has formed a shell on top of the nickel core, significantly reducing the amount of palladium compared to the previous versions of these catalysts. The new catalyst increases oxygen activity roughly three times more than state-of-the-art platinum catalysts. Figure 2 shows the performance of these catalysts in a 5 cm² fuel cell membrane electrode assembly (MEA) under the industry standard operating conditions and accelerated stress test (AST) protocol. These MEAs show very good durability under the AST.

Remaining challenges include optimizing the electrode to improve the hydrogen/air performance to match the state of the art MEAs, and increasing development volumes of these catalysts to meet industry-level advanced needs.
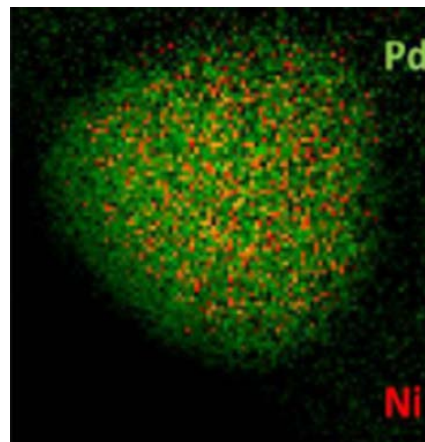
Figure 1. High-resolution transmission electron microscopy image shows that the palladium forms a shell on top of the low-cost nickel core.
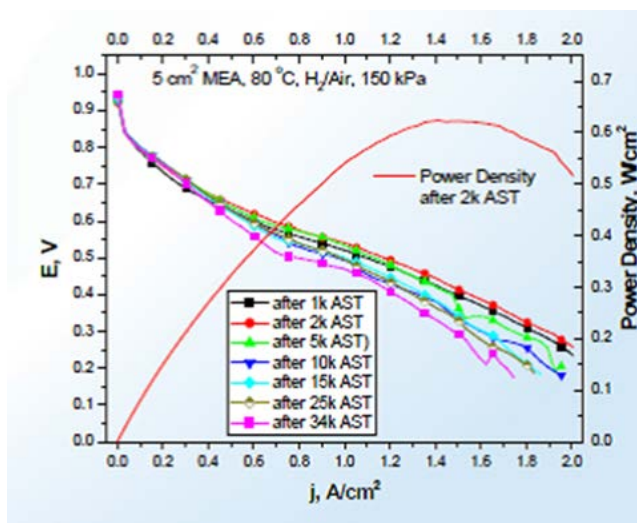
Figure 2. Hydrogen/air polarization curve at U.S. Department of Energy's recommended conditions using the platinum monolayer catalyst on a palladium shell with a low-cost core, showing very good durability.

Improved Catalyst Layer through Engineered Design

New catalyst layer structure shows performance approaching that of an automotive baseline catalyst layer, with promise for further improvement.

Los Alamos National Laboratory

While many components of automotive proton exchange membrane fuel cell (PEMFC) stacks have become more engineered and better designed to meet specifications, catalyst layers still remain relatively ill-defined. Catalyst layer structures are often the consequence of the ink processing by which they are made, rather than how they are designed and engineered. Given the extraordinary amount of chemical kinetics, proton transport, heat transport, and gas transport functionality that resides within catalyst layers, engineering better catalyst layers is a substantial opportunity for improving the performance and durability of PEMFCs.

Los Alamos National Laboratory (LANL) recognized that proton transport in a catalyst layer could be improved by engineering multiple phases as part of an engineered ionomer topology (EIT). As shown in Figure 1, the EIT was designed to include a scaffold phase that would connect the tin film ionomer phases that surround catalyst agglomerates. The thin film phases can now be reduced in thickness, which would enhance oxygen transport to the catalyst surface, thereby increasing power.

Originally the scaffold phase was to be comprised of ionomer nanofibers from electrospinning, but the nanofiber diameters were too large. Instead, LANL generated the scaffold phase by coating ionomer onto multi-walled carbon nanotubes (MWCNTs). Next, using a lower Nafion content in the catalyst ink along with ionomer-coated MWCNTs, catalyst layer decals were made and then transferred through hot-pressing onto the membrane. Figure 2 shows that despite lower electrochemical surface area, the EIT membrane electrode assembly (MEA) performed nearly equivalent to a baseline MEA from General Motors LCC's (GM) with the same platinum loading.

Figure 1. Each side chain contains two super acid groups: one imide and one sulfonic acid.

Figure 2. Polarization for the EIT MEA at low platinum loading is nearly equivalent to that of an automotive baseline MEA.

Spectroscopic Method Enables Visualizing Ionomer Dispersions in Fuel Cell Electrodes

New techniques enable ionomer mapping across full electrode cross-section, such that uniformity of the ionomer distribution can be assessed and quantified at nanometer-scale spatial resolution.

Oak Ridge National Laboratory

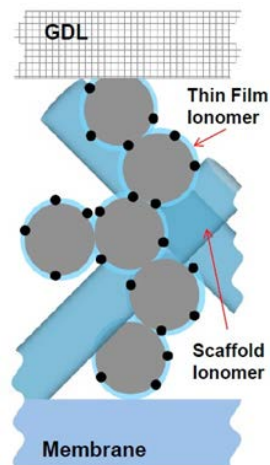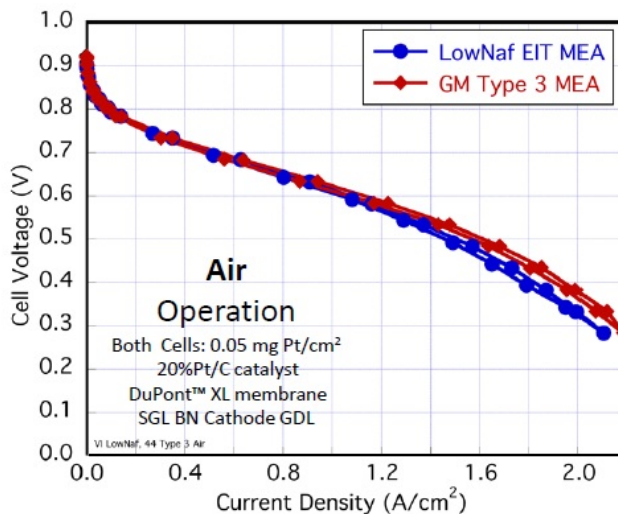The ionomer thin-film layer plays a critical role in determining fuel cell performance by controlling ionic and mass transport, as well as electrochemical kinetics, within fuel cell catalyst layers. Being able to see how the ionomer is distributed in the catalyst layer is key to optimizing the catalyst layer structure and composition. Characterizing the uniformity of ionomer thin-films, as well as quantifying the ionomer distribution and continuity within catalyst layers, has proven challenging because the polymer undergoes extremely rapid chemical degradation during analysis using traditional high-resolution transmission electron microscopy (TEM) imaging and spectroscopy techniques. Oak Ridge National Laboratory (ORNL) has been the first in the world to demonstrate up to 100 times faster detection times, resulting in minimal ionomer loss and accurate imaging within the catalyst ionomer layers.

ORNL has conducted an in-depth evaluation to determine the best practices for conducting microscopy studies aimed specifically at elucidating the nature of the ionomer thin-film network within catalyst layers, without causing significant damage to the ionomer during TEM analysis. Established protocols include conducting the ionomer analyses with the sample held at cryogenic temperatures, and operating the TEM under low-electron dose conditions and high accelerating voltages. Recently, analytical studies have been further enabled by the development of large solid-angle energy dispersive X-ray spectrometry (EDS) systems, which have extremely high X-ray collection efficiencies and a 10 to 100-fold decrease in data collection times.

These analytical studies have focused on understanding ionomer aggregation phenomena in catalyst layers as a function of catalyst ink preparation methods, and the quantification and distribution of the ionomer and its morphology

(thick layers, thin films, or aggregates) across the full thickness of the catalyst layers. The ultimate goal of this work is to correlate the observed ionomer distributions with ink and membrane electrode preparation methods, specific electrode materials used, and fuel cell performance. These capabilities are now available to the fuel cell community to use through ORNL's Materials Characterization Center, with up to 50% funding support available from the U.S. Department of Energy.
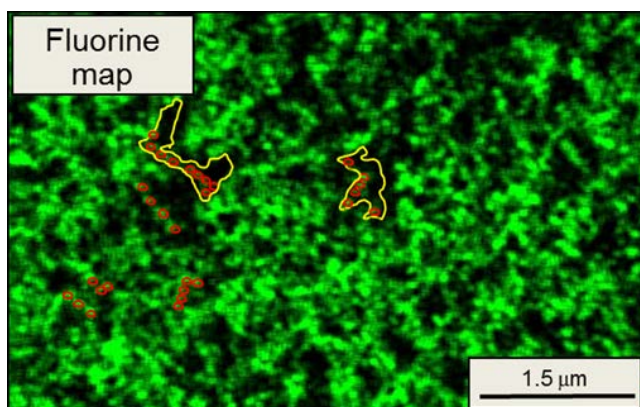
Figure1. Fluorine map using advanced EDS system shows distribution of ionomer across a 5µm thick uniform cathode catalyst layer. Ionomer aggregates are observed, most notably at the top of the catalyst layer. Ionomer is shown in green. Red circles denote linked chains of aggregates. Secondary pores are shown in yellow.

Durable Platinum Alloy Cathode Catalysts Demonstrated

Highly active hybrid cathode catalyst shows excellent support stability and catalyst durability.

University of South Carolina

Cathode durability, cost, and performance are some of the key issues preventing the commercialization of polymer electrolyte membrane fuel cells for automotive applications. Catalyst and catalyst support degradation during startup and shutdown and potential cycling experienced during operation limit catalyst lifetime. The platinum (Pt) alloy development project at the University of South Carolina (USC) has developed a highly active and stable catalyst/catalyst support system that retains its activity after accelerated testing to simulate startup/shutdown and drive cycle voltage cycling. These catalysts have achieved a mass activity of 0.41 A/mg Pt, approaching the U.S. Department of Energy's activity target of 0.44 A/mg Pt, while losing less than half of the target 30 mV at high power conditions (1.5 A/cm²) after 5,000 accelerated stress test (AST) cycles, simulating highly degrading conditions at startup/shutdown (see Figure 1).
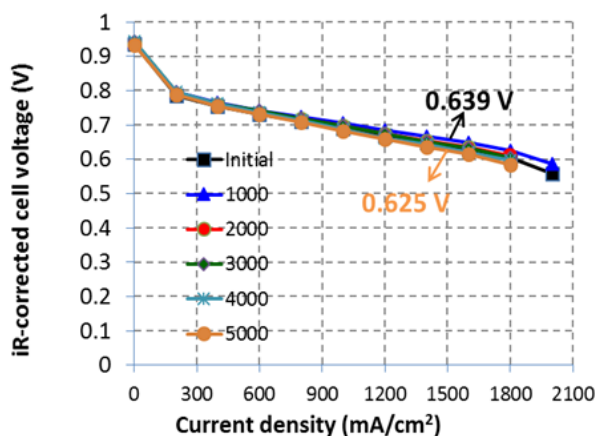
Figure 1. Comparison of hydrogen air fuel cell performance of 30% Pt*/ACCS catalyst subjected to 5,000 AST cycles between 1.0 V and 1.5 V at 500 mV/s.

USC's technology is based on a two-step patented process. In the first step, activated carbon composite catalyst supports (ACCS) are prepared that are chemically and electrochemically stable at high potentials, low pH, and high-temperatures; and exhibit kinetic activity for the oxygen reduction reaction at a potential similar to that of a Pt catalyst. The ACCS shown in Figure 2 was synthesized with optimized surface area, porosity, pore-size and pore-size distribution; hydrophilic/hydrophobic ratio; structural properties (amorphous/crystalline ratio); number of catalytic active sites; Pt-support interaction through inclusion of active surface functional groups; and transition metal necessary for the formation of Pt encapsulated within the graphitic carbon structure.
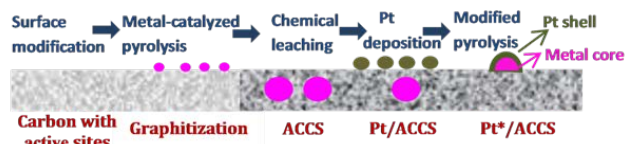
Figure 2. Schematic of the USC Pt*/ACCS catalyst synthesis.

In the second step, a Pt catalyst with a compressed Pt-lattice is synthesized through a USC-developed annealing procedure that controls the particle size during annealing and forms monolayers of compressed Pt by diffusing cobalt atoms present in the support into Pt, which is deposited on ACCS support. The Pt/ACCS shows high mass activity, excellent support stability, and enhanced catalyst durability under AST conditions.

Materials

Advanced Oxidation to Improve Carbon Fiber Manufacturing Process Throughput

Plasma oxidation oven systems can significantly reduce the mass throughput bottleneck of carbon fiber manufacturing within one-third of the manufacturing floor space while achieving a 25% reduction in energy usage and a 20% reduction in manufacturing cost.

Oak Ridge National Laboratory

Plasma oxidation is a newly developed technology that addresses the mass throughput bottleneck of the carbon fiber manufacturing process – the oxidation/stabilization stage. That processing stage is necessary to make the precursor infusible and able to tolerate the high temperatures required in the subsequent carbonization stage. Compared to conventional oxidation, this technology has been shown to make a better product (e.g., increased tensile strength using the same precursor) and oxidize three times faster. It also uses only approximately 25% of the energy per pound of oxidized fiber, takes up significantly less space (see Figure 1), and reduces the carbon fiber manufacturing costs by 20%. The technology has been successfully demonstrated at 1 annual metric ton (aMT), but can be scaled to full production levels of 1,500 aMT and greater.

A project involving Oak Ridge National Laboratory (ORNL) and RMX Technologies successfully completed development work on the plasma oxidation technology. In addition to meeting all project milestones, RMX processed several industrial clients' precursors in the 1 aMT plasma oxidation oven at RMX, exceeding expectations. The 1 aMT oven has hundreds of operating hours since it came online in the Spring of 2014.

RMX Technologies has recently executed a license with ORNL to manufacture and sell plasma oxidation ovens. RMX has established a subsidiary, 4M Industrial Oxidation, that is leading the commercialization effort in partnership with C.A. Litzler, an established conventional oxidation oven manufacturer. Based on feedback from the carbon fiber industry, 4M and Litzler have already begun scaling the technology from 1 to 175 aMT in privately-funded endeavors.

Conventional and Advanced Oxidation Oven Systems
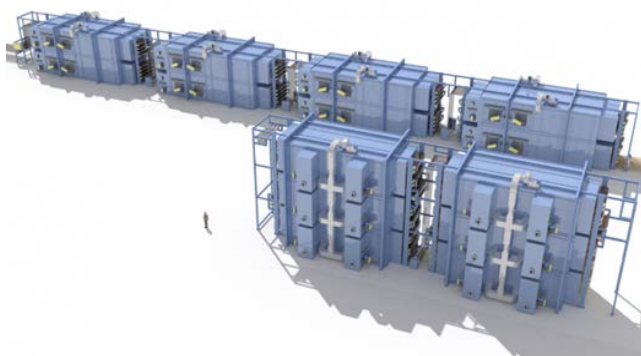
Figure 1. A conventional oxidation oven system (upper) and a plasma oxidation oven system (lower) – both at a nameplate capacity of 1,500 aMT. Illustration provided in part by C.A. Litzler. The plasma oven's processing length is approximately one-third the length of comparable conventional ovens.

Cast Bonding of Iron to Aluminum Optimization

Project seeks to achieve consistent cast bonds between steel inserts and aluminum castings equal to or exceeding the shear strength of the aluminum alloy.

U.S. Automotive Materials Partnership LLC

The tool box of fastening solutions for aluminum (Al) components to steel structures and vice-versa is limited in today's multi-material vehicles. For instance, there are no known economically attractive processes to create a metallurgical bond between Al and iron components. Riveting and threaded fastening are reliable but not always attractive to the designer or manufacturer due to weight, quality, productivity, warranty and reliability considerations. A robust fastening solution that results in a metallurgical bond would be a very attractive addition to the multi-material assembly tool box.

Previously-completed concept feasibility work showed that introducing ultrasound to ferrous inserts in a mold for cast Al can result in a metallurgical bond between the insert and the Al casting with no loss in productivity. Physical test results indicated the failure mode of these joints was tearing of the Al, not failure in the interface.

Technical hurdles were identified in the concept feasibility work. The most pressing hurdle identified was proving that the process worked in a steel mold. A subsequent project established that the ultrasonic cast bonding technology worked in a steel mold without the casting attaching to the die surface. The project was completed, indicating that bonding of steel to Al was achieved successfully without bonding to the steel mold.

The most recently completed work was successful, but the corresponding bond strengths varied. From the data generated it was difficult to establish a clear cause and effect relationship due to the variation of several parameters at the same time. Optimization, still in the small laboratory size mold, appeared to be in order before scaling up the process. The current project's focus is a well-planned and well-controlled design experiment, where the influence of each of the parameters is evaluated for better understanding of the formation of microstructures observed in the castings.

The successful development of this technology will result in a significant reduction in parts and material, as well as machining for drilling, tapping and press fitting. Applications exist in both body structures and powertrain. In addition, there is the potential to eliminate the Al sleeves that capture iron cylinder bore liners, resulting in engines that are shortened by up to two inches (see Figure 1). The estimated mass savings could exceed 30 pounds of Al and steel per vehicle.

The work completed in 2015 has identified optimal manufacturing parameters for a gel couplant between the ultrasound probe and steel insert and for a mechanical (threaded) couplant. The remaining work in 2016 will focus on a magnetic couplant.
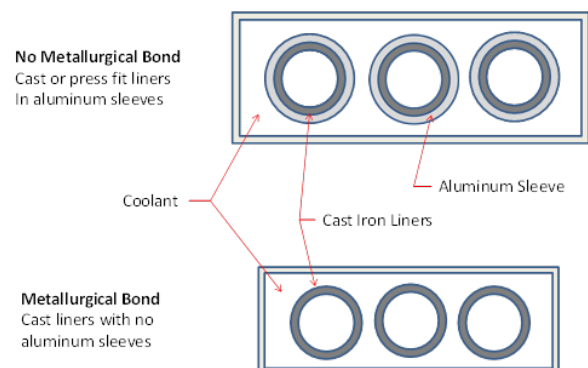

Figure 1. Top, cross-section of cast liners with Al sleeves. Bottom, cross-section of cast liners with no Al sleeves, potentially resulting in engines that are up to two inches shorter.

Durability of Magnesium-to-Steel Joints

Durability of novel joining technique demonstrated and modeled with acceptable accuracy.

U.S. Automotive Materials Partnership LLC

Incorporating dissimilar metals, such as galvanized steel and aluminum, into primarily die-cast magnesium structures by novel joining methods has been reported previously as a part of the final phase of the Magnesium Front-End Research and Development program. Greater integration of magnesium alloys into vehicle assemblies could advance the weight reduction goal of the U.S. DRIVE's Materials Technical Team for improving vehicle fuel efficiency.

The joining of die-cast magnesium to high-strength galvanized steel is particularly challenging, given the metallurgical complexities of such joints, as well as the opportunity for galvanic coupling and associated corrosion of the magnesium member in the presence of electrolytes. The most recent report on this effort described the adaptable insert welding (AIW) process employed to secure protectively-coated, high-strength steel to AM60B die-cast magnesium via use of a special magnesium insert plug and conventional resistance welding.

Once the AIW joining technology was developed, the next challenge was determining durability (fatigue) characteristics under vehicle load conditions and engineering methods for predicting such joint lifetimes in the structures of interest. The methodology for joint durability characterization had five elements:

1. Developing the capability to produce both lap and coach peel joints at the coupon level between materials of interest in construction;
2. Determining the fatigue behavior of coupon assemblies under these well-defined loading conditions;
3. Using the finite element method (FEM) to deduce the structural stress within the joint regions via the application of either tie or area contact representations of the joints on a macroscopic scale;
4. Predicting joint durability in an actual structure, using FEM and known applied loads to deduce structural stresses at the joint locations; and
5. Experimental determination of joint or structure fatigue life for various loadings.

Figure 1 illustrates the correlation between predicted and measured lifetimes for a single loading orientation (designated 'Y') of AIW joints connecting an upper steel rail to a magnesium die casting. Predicted lifetimes are within a factor of three, which is considered to be appropriate and highly acceptable for these types of analyses.
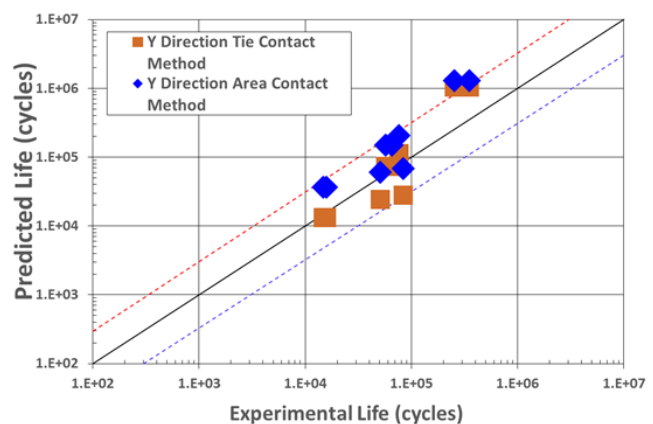

Figure 1. Correlation plot for predicted and experimental fatigue lifetimes of AIW joints between high-strength steel and die-cast magnesium, in demonstration structures using either area or tie contact finite element representations of the joint. Dashed lines indicate +/- factor of three variations.

New Experimental Procedure to Assess Transformational Kinetics in Third-Generation Advanced High-Strength Steel

New experimental procedure will improve the accuracy of the integrated computational material model for third-generation advanced high-strength steels and energy management applications.

U.S. Automotive Materials Partnership LLC

The project's objective is to demonstrate the applicability of an integrated computational materials engineering (ICME) approach for developing and deploying third-generation advanced high-strength steels (3GAHSS). The approach is to link and integrate established computational material models at different length scales, which are calibrated against experimental 3GAHSS data. The 3GAHSS alloys tested in this project, with their very fine grain size and metastable retained austenite, present significant challenges in measuring the constitutive material properties needed for model calibration. The ICME 3GAHSS project has developed a novel experimental methodology that enables it to align ICME model predictions with 3GAHSS experimental data.

The ICME model output is a material flow curve that is the summation of the combined contributions of the microstructural phases (ferrite, martensite, bainite and/or austenite) present. The initial ICME model did not account for phase transformations as a function of strain. 3GAHSS (10% manganese (Mn) steel) produced by the project for model calibration has a significant percentage of retained austenite that when strained transforms to martensite. The change in volume fractions of austenite and martensite resulted in an ICME predicted flow curve for this material that deviated from experimental results. Accounting for phase transformation was necessary to calibrate the 3GAHSS ICME model.

Prior approaches to experimentally characterize austenite to martensite phase transformation involved multiple interrupted tension tests coupled with local strain measurements using a digital image correlation (DIC) technique and microscopy. The technique accurately measures retained austenite with strain and remains the preferred option for complex loading, albeit time consuming and requires extensive DIC data processing.

To address these drawbacks, the project developed a novel experimental methodology that for the first time couples tensile testing with DIC and high-energy X-ray diffraction. Working at Argonne National Laboratory's Advanced Neutron Source, gridded 3GAHSS coupons were strained in a tensile fixture. DIC enables local response to strain to be assessed in the region where X-rays are applied. Figure 1 shows the stress/strain curve for the 10% Mn steel with corresponding retained austenite volume fraction (RAVF).

This procedure has enabled faster characterization of material properties essential for the transformational kinetics modeling. The ICME code, incorporating the transformation kinetics, provides more accurate prediction of material flow curves, resulting in better prediction of 3GAHSS component forming and crashworthiness behavior.
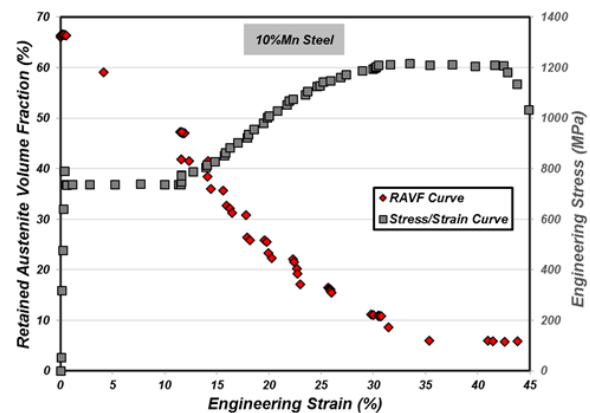

Figure 1. A plot of the engineering stress/strain curve superimposed on the RAVF curve.

Validation of Carbon Fiber Composite Material Models for Automotive Crash Simulation

The project selected and characterized materials, and completed test component design, for validation of carbon fiber material models to enable the high-volume use of lightweight carbon fiber composites in structural crash and energy management applications.

U.S. Automotive Materials Partnership LLC

This four-year validation project has completed the third year of an extensive analytical modeling and physical testing program to validate commercial constitutive models implemented in crash codes (i.e., ABAQUS, LS-DYNA, PAM-CRASH and RADIOSS), and two newer crash models developed by academic partners. These include a meso-scale representative unit cell (RUC) model[1] (University of Michigan (UM)) and a micro-plane RUC model[2] (Northwestern University). The project team is comprised of researchers from the U.S. Automotive Materials Partnership's original equipment manufacturers and academia, representing the computer-aided engineering, materials testing, and crash testing functions, as well as automotive design and engineering suppliers, composite manufacturers, material suppliers, and test laboratories.

The project's goal is to validate material models for reliably designing structural automotive carbon fiber composites for crash applications. The team chose a front bumper beam and crush-can (FBCC) subassembly application to validate the material models by developing a composite FBCC that can be shown to absorb impact energy equivalent to a baseline steel FBCC under various crash-loading modes, and comparing its actual performance to simulations.

During year three, the project team finalized the FBCC design, consisting of a bumper beam and two crush cans, with each dodecagonal crush can being made of two symmetrical halves and bonded and riveted alongside flanges (Figure 1). The team also finalized the predictions of crush can load capacities in the academic RUC and micro-plane models, and

integrated UM's RUC model into the PAM-CRASH commercial software code. The design and initial methodology to join the crush can to the beam has also been developed with several adhesive/rivet systems being tested.

Figure 1. Carbon fiber FBCC, made from two compression-molded crush cans and a thermoset carbon fiber bumper beam with fabric C-channel and carbon SMC ribs.

Tooling was designed and fabricated for preforming and molding the crush cans for a thermoset epoxy/carbon fiber material system. The first molding trials for the beam used innovative one-shot compression molding of a woven C-channel beam with carbon sheet molding compound (SMC) ribs, while the crush cans were predominately woven with SMC front and rear flanges. The first FBCCs have been molded and assembled, and an initial crash test was successfully carried out. Plans are underway for molding with thermoplastic systems, and non-destructive engineering methods developed earlier in the project are being trialed. After crash testing in six load cases, the physical results will be compared with the analytical predictions.

---

[1] Song S, Waas AM, et al., <u>Composites Science and Technology</u>, 67, pp 3059-3070, 2007.

[2] Caner, F.C., et al., <u>Journal of Engineering Materials and Technology</u>, 133, pp 1-12, 2011.

Vehicle Systems Analysis

In-Depth Technology Assessment of Electric Vehicles

Quality, independent and public data and analysis are rare and too expensive for most research institutions to generate. This project provides the foundational data on which innovation is built. It also establishes technology trends, develops simulation models, and informs the development of test procedures.

Argonne National Laboratory

The Advanced Powertrain Research Facility benchmarked nine different battery electric vehicle models and three plug-in hybrid electric vehicles. The comprehensive evaluation of the fully instrumented vehicles went well beyond standard certification tests, and was done across temperatures ranging from 0°F to a sunny 95°F in a thermal chamber to establish energy consumption, electric range, maximum performance, and charging efficiency at the vehicle level. Researchers measured and analyzed at the component level the performance and efficiency of many specific powertrain technologies, battery systems, chargers, and climate control systems

Figure 1 illustrates an example of this activity's findings. It quantifies the variation in electric range depending on driving cycle, ambient temperature and accessory use. On average, compared to 72°F, the range penalty in city driving is 51% at 20°F and

18% at 95°F, due mainly to the power consumption of cabin heating or cooling. Cabin and powertrain thermal preconditioning during vehicle charging can increase the city range at 20°F by 5%. Heat pump systems are most active at off-cycle test conditions, such as 40°F test temperature, providing real-world range benefits.

The benchmark data and analysis serve to establish technology trends, inform U.S. Department of Energy research target setting, develop and validate simulation models, and inform technology neutral test procedures development. For instance, the BMW i3 range extender was difficult to test via the standard SAE J1634 BEV procedure, which must be revised to stay relevant to evolving technologies.

A select data subset is posted to a public web portal (www.anl.gov/d3), and additional data sets are available from Argonne National Laboratory by request.

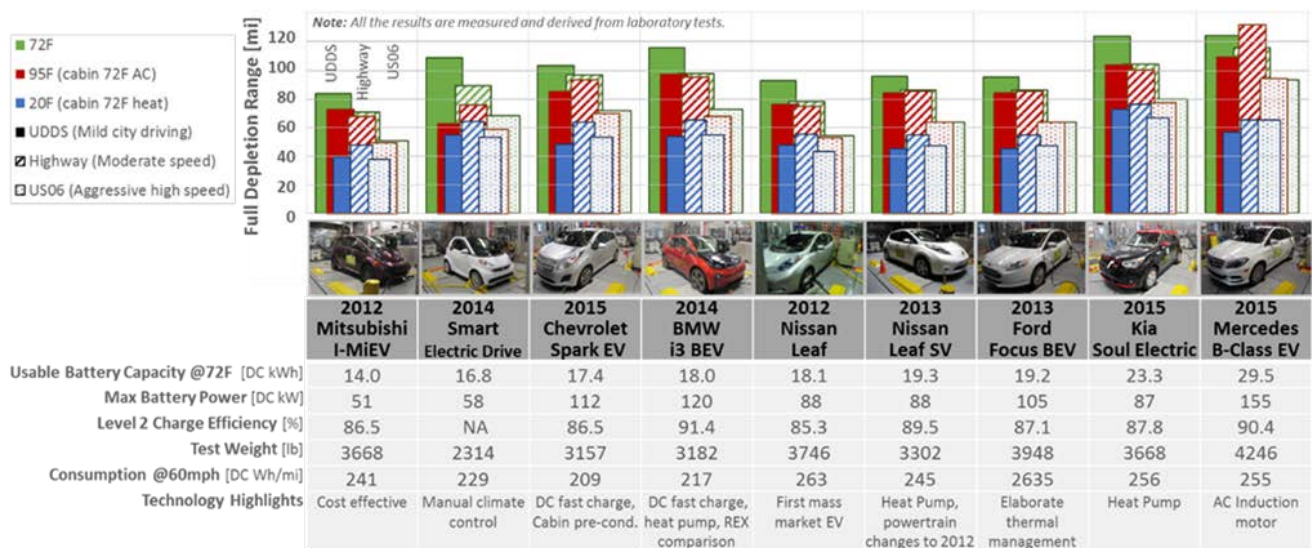|	2012 Mitsubishi I-MiEV	2014 Smart Electric Drive	2015 Chevrolet Spark EV	2014 BMW i3 BEV	2012 Nissan Leaf	2013 Nissan Leaf SV	2013 Ford Focus BEV	2015 Kia Soul Electric	2015 Mercedes B-Class EV
Usable Battery Capacity @72F [DC kWh]	14.0	16.8	17.4	18.0	18.1	19.3	19.2	23.3	29.5
Max Battery Power [DC kW]	51	58	112	120	88	88	105	87	155
Level 2 Charge Efficiency [%]	86.5	NA	86.5	91.4	85.3	89.5	87.1	87.8	90.4
Test Weight [lb]	3668	2314	3157	3182	3746	3302	3948	3668	4246
Consumption @60mph [DC Wh/mi]	241	229	209	217	263	245	2635	256	255
Technology Highlights	Cost effective	Manual climate control	DC fast charge, Cabin pre-cond.	DC fast charge, heat pump, REX comparison	First mass market EV	Heat Pump, powertrain changes to 2012	Elaborate thermal management	Heat Pump	AC Induction motor

Figure 1. Battery electric vehicle performance measured on a chassis dynamometer in a thermal chamber.

Route-Based Energy Management

With route-based energy management, a connected vehicle can adapt its control to the planned itinerary to improve fuel efficiency.

Argonne National Laboratory

In a vehicle, the vehicle control unit commands the different vehicle components to minimize the energy consumed while providing the power at the wheel requested by the driver. For plug-in hybrid electric vehicles (PHEVs), the system must decide whether to use the battery or the engine for propulsion, when to turn the engine on, and how to use it in conjunction with the electric machines. Classic energy management is based on the present state of the system. However, advanced algorithms based on control theory with knowledge of future vehicle speed can lead to energy savings.

To quantify the energy impact, researchers at Argonne National Laboratory (ANL) have developed a route-based energy management (RBEM) concept (Figure 1). At the beginning of a trip, the origin, destination and itinerary can be known from the navigation unit, either through user input or through pattern recognition of previous routes. Information about the route is then used to predict a precise speed profile. The vehicle controller can then be optimally tuned using the predicted speed. The research team made significant strides in the speed prediction and vehicle control areas.

One critical achievement is the speed prediction algorithm. ANL researchers have designed a method to generate a realistic second-by-second vehicle speed profile prediction for the future route based on real-world driving data analysis. The profiles are also specific to the particular route selected, thanks to the information about speed limits, traffic speed and intersection control from the automotive grade digital map, provided by HERE.

The team implemented the RBEM concept for a Toyota Prius PHEV using Autonomie, a vehicle simulation environment developed at ANL.

In the case of a PHEV, preliminary studies have shown that the RBEM can save fuel (5% to 10%) for longer trips, when there is not enough electrical energy to cover the entire trip on electricity alone. The controller then intelligently assigns battery energy to the areas where the engine is the least efficient (e.g., urban and congested zones).

ANL researchers will continue to refine this work, particularly to understand the sensitivity of the RBEM to prediction and driving uncertainties.
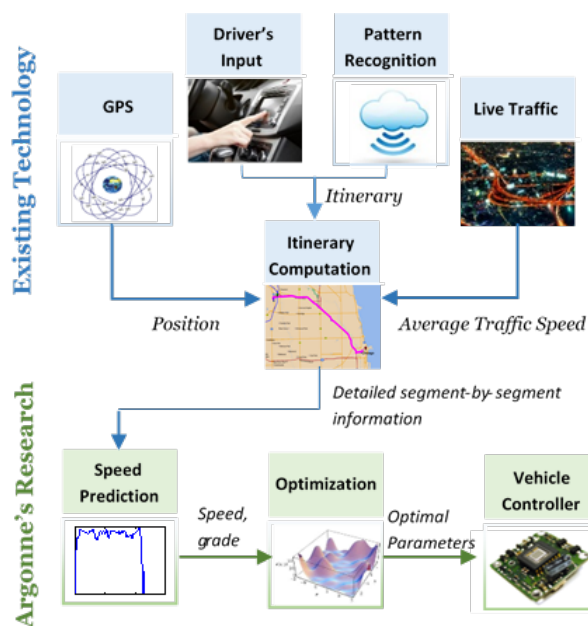

Figure 1. Conceptual view of RBEM.

Analyzing Real-World Vehicle Efficiency Benefits

Novel application of big-data tools estimates potential fuel savings of "off-cycle" technologies equivalent to taking 2.5 million vehicles off the road.

National Renewable Energy Laboratory

Laboratory testing over standardized drive cycles reveals important information about vehicle fuel efficiency but is unable to predict fuel savings from "off-cycle" technologies, such as thermal retention or connected and automated vehicle innovations. To address this, the National Renewable Energy Laboratory (NREL) generated a thermally sensitive powertrain model (validated by data from Argonne National Laboratory), and developed an analytical methodology to link driving behavior, road network, elevation profile, traffic volume, temperature, and solar radiation data (Figure 1).

NREL implemented a computationally efficient methodology to calculate vehicle fuel efficiency across the full range of localized real-world conditions that a vehicle may encounter in the United States. To calculate overall average fuel efficiency, NREL weighted each localized efficiency value by the total amount of driving that occurs under each condition nationally. Repeating this process first for a baseline condition and then for a situation where a vehicle employs an "off-cycle"

technology enables the combined data collection and modeling process to capture a given technology's different impacts under different localized driving situations. Then, uneven situational benefits are appropriately combined based on the typical amount of driving each situation represents considering U.S. driving data and a typical meteorological year.

With this analytical framework, public and private stakeholders can objectively evaluate the aggregate benefit of off-cycle efficiency technologies, making them easier to commercialize. Early results indicate that real-world benefits for some thermal retention technologies could exceed 1%. If broadly implemented, this seemingly modest fuel savings would have the aggregate impact of taking 2.5 million vehicles off the road. Ongoing work in fiscal year 2016 will include further refining the methodology, validating against on-road data collection, and applying to other off-cycle technology scenarios.
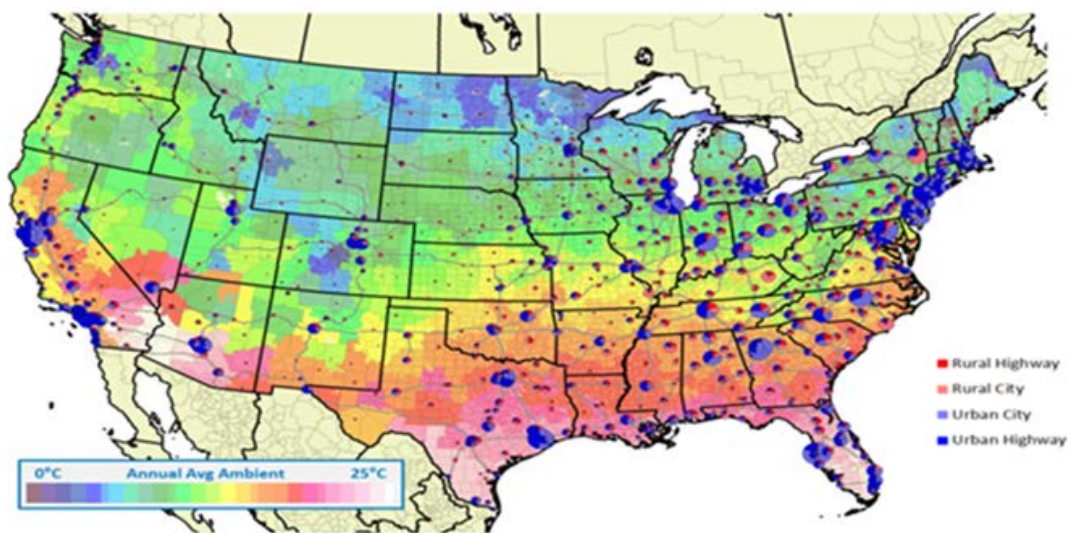

Figure 1. NREL's analytical methodology considers relative distributions of driving miles in different traffic conditions, overlaid with typical weather conditions over a year.

Reducing Cabin Heating Loads in Electric Vehicles

Zonal cabin heating strategy demonstrates potential for 7.1% increase in electric vehicle range.

National Renewable Energy Laboratory

Electric vehicles (EVs) require cabin climate control for passenger thermal comfort and safety. Heating and cooling can have a large negative impact on the EV's maximum driving range, presenting a major challenge for many drivers and a barrier to widespread adoption. Using electric resistance heaters for cabin conditioning takes valuable battery energy away from propulsion. Oversizing traction batteries to overcome range limitations is too costly to be a viable solution. Therefore, it is critical to minimize climate control loads in EVs to maximize vehicle range.

Over the past three years, National Renewable Energy Laboratory (NREL) researchers investigated climate control load reduction strategies using complementary experimental and analytical techniques. NREL collaborated closely with Ford, which provided two Focus Electric vehicles and engineering support. Thermal soak and transient tests were conducted with instrumented test vehicles to measure cooling and heating power requirements. Computer modeling and analysis were used to explore load reduction strategies to estimate impact on EV range.

NREL researchers completed cold-weather, outdoor thermal testing to evaluate zonal heating concepts, designed to save energy by warming the occupant and not the entire car (see Figure 1). The test configuration incorporated air flow and heated surfaces for the driver location in the vehicle cabin. The test results demonstrated the potential to decrease energy consumption by more than 28.5% while maintaining driver thermal comfort during warm-up. This energy savings increases the vehicle range by 6.9% to 18.7% compared to a vehicle with a baseline heating strategy. The national weighted improvement in range is 7.1% over the baseline

heating strategy, which is a 33% reduction in range penalty due to heating.

The range improvement estimates were based on 20-minute drive simulations using heating power appropriate for 32°F. The range improvements due to zonal strategies in moderate environments and for longer drive cycles will be lower.

Using zonal heating strategies in conjunction with increased insulation, a heat pump, or thermal preconditioning can be part of a combined strategy to minimize the impact of heating on EV range. Occupant-based thermal comfort control of heating, ventilation, and air conditioning (HVAC) could reduce energy consumption further. NREL is continuing to work closely with the automotive industry to develop and improve these technologies and quantify the benefits. Energy savings from HVAC load reduction solutions translate directly into increased energy for vehicle propulsion, which improves driving range and can lead to wider EV adoption.

Figure 1. Cold-weather testing of the Ford Focus Electric at NREL's outdoor vehicle test pad.

Vehicle Simulations Predict Future Fuel Economy Improvements from Advanced Combustion Engines

Vehicle systems simulations using experimental engine data predict a 30% fuel economy improvement compared to baseline gasoline port fuel injection engines common in the marketplace.

Oak Ridge National Laboratory

There are a number of promising advanced combustion modes currently in the research and development (R&D) stage that have demonstrated high fuel efficiencies and low engine-out emissions during steady-state operating conditions. However, it is difficult to predict the impact on real-world light-duty vehicle fuel economy from measurements taken only during steady-state engine operation in the lab. Using vehicle systems simulations to estimate the fuel economy of these advanced combustion modes over a range of speeds and loads is critical for identifying promising paths for improving fuel economy and lowering emissions.

Researchers at Oak Ridge National Laboratory used the vehicle simulation tool, Autonomie, to simulate near real-world driving conditions and obtain fuel economy estimates from advanced combustion modes, such as reactivity controlled compression ignition (RCCI). RCCI is a low-temperature combustion mode that uses diesel fuel and gasoline in an engine simultaneously. Recent simulations have shown that gasoline and diesel RCCI has the potential to improve fuel economy by more than 30% compared to the same base vehicle using a 2009 port fuel injection (PFI) gasoline engine baseline both in terms of miles per gallon of fuel used (MPG) and energy corrected fuel economy (miles per gasoline gallon equivalent (MPGGE)), as shown in Figure 1.

To generate these fuel economy estimates, experimental engine performance maps were created from engine dynamometer experiments in the lab. These engine maps were then used in the vehicle systems simulations to model the performance of a virtual advanced combustion vehicle over the standard drive cycles used for fuel economy and emissions certification. These simulations provide estimates of fuel economy in terms of MPG over a drive cycle.

The ability to incorporate prototype combustion engine data into physics-based simulations at the vehicle level accelerates the understanding of the engineering challenges of implementing advanced combustion modes. The simulations are also valuable in predicting trends in emissions. These vehicles system findings support the U.S. Department of Energy's Advanced Combustion Engine and Fuel and Lubricant Technologies R&D programs.
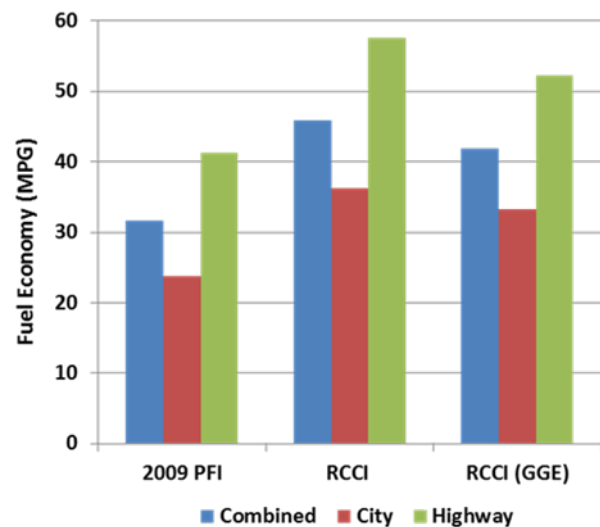

Figure 1. Fuel economy estimates for combined light-duty drive cycle along with city and highway portions for RCCI compared to 2009 PFI baseline in MPG and MPGGE (labeled GGE).

Codes and Standards

Successful Field Trials of Hydrogen Safety Sensor

Derived from proven automotive exhaust sensor technology, the electrochemical, mixed-potential hydrogen sensor successfully completed hydrogen station field trials with no baseline drift.

Los Alamos National Laboratory and Lawrence Livermore National Laboratory

Since 2008, Los Alamos National Laboratory (LANL) and Lawrence Livermore National Laboratory (LLNL) have been collaborating to develop low-cost, durable, and reliable hydrogen sensors based on zirconia oxygen ion-conducting solid electrolytes (see Figure 1). In 2015, field trials at a California hydrogen fueling station showed impressive results in key metrics such as sensitivity, response time, and resistance to interference from non-hydrogen gas species (despite being situated outdoors in a heavily congested city environment).

Hydrogen sensors are recognized as an important device in implementing safety functions, such as indicating unintended hydrogen release, activating mitigation strategies to preclude the development of hazardous situations, and activating alarm systems and communications to first responders. Sensor systems may even be tasked with autonomous initiation of a system shutdown.

The technology behind this new hydrogen sensor is derived from a hugely successful automotive low-cost lambda oxygen sensor. However, unlike that sensor, this mixed-potential electrochemical hydrogen sensor is based on differential electrode kinetics of the hydrogen oxidation reaction and oxygen reduction reaction between specific electrode materials and structures. LANL has developed sensor constructs that use ceramic materials with stable and reproducible sensor interfaces. While simple and inexpensive, the sensor is chemically and physically robust for operation in harsh environments. Long-term durability testing data confirm the absence of sensor baseline drift, and false positives and false negatives.

During field trials, the sensor successfully responded to hydrogen releases that occurred during venting of the supply hose prior to its disconnection from a fuel cell vehicle (FCV). These field trials were a significant step on the path from lab development towards "real-world" commercialization. An expansion of field trials is planned for 2016, funded by the State of California and led by LLNL.
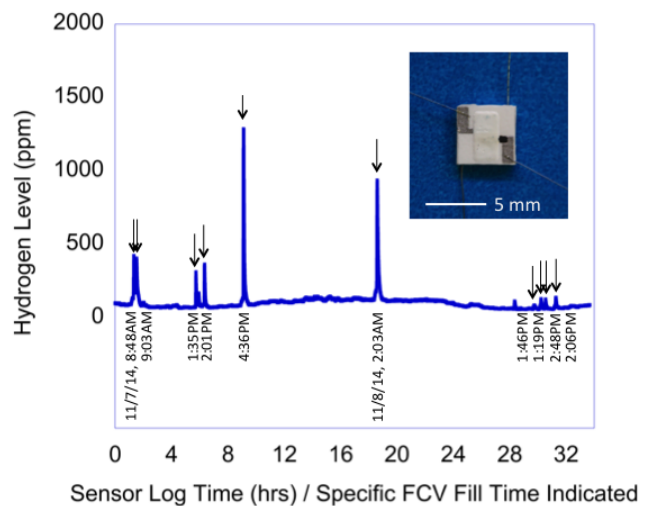
Figure 1. Sensor responses to hydrogen captured during outdoor testing at a California hydrogen filling station. Hydrogen releases of non-consequential levels are due to normal venting of the supply hose before the FCV disconnects.

New Hydrogen Tools Portal Shares Safety Knowledge

Transformative web-based tool facilitates easy access to many hydrogen safety resources from a single website viewable on desktop and mobile devices and is focused on content for specific user groups.

Pacific Northwest National Laboratory

The entire hydrogen industry benefits when credible and reliable safety information is shared from a trustworthy source. In 2015, the Pacific Northwest National Laboratory (PNNL) developed the Hydrogen Tools Portal (http://h2tools.org) for disseminating hydrogen safety knowledge to critical user groups (see Figure 1). PNNL responded to a diverse set of hydrogen user groups that indicated a need for a central portal for integrating and disseminating safety information. This portal is expected to contribute significantly to hydrogen commercialization. It will help inform those tasked with designing, approving, or using systems and facilities, as well as those responding to incidents.

The Hydrogen Tools Portal incorporates a variety of safety knowledge resources focused on lessons learned, best practices, codes and standards, compatibility of materials, and training, among other topics. The Portal also serves to highlight the work and capability of the Hydrogen Safety Panel and to bring visibility to the Hydrogen Fueling Infrastructure Research and Station Technology project resources. The Portal's innovative workspaces uniquely configure site content for specific user groups, including authorities having jurisdiction, first responders, project proponents, risk managers, researchers and equipment operators.

The significant benefits of this approach include easy access to multiple safety resources from one location and the ability to search for specific content across all resources. A responsive design allows the resources to be accessed from desktop and mobile devices. Access to integrated safety resources from a single, trustworthy source increases visibility and value through a "one-stop-shop" approach. Providing a consistent set of accurate and up-to-date safety information will help to remove unnecessary roadblocks and also foster public confidence in the use of hydrogen and fuel cell vehicles.

The approaches taken for the Portal are creating a rich environment for learning and applying safe hydrogen practices. With its current resources, site features and design flexibility, the Hydrogen Tools Portal goes a long way to achieve its goal of sharing safety knowledge. Ongoing user feedback with the intent to add additional resources will help further the Portal's value as a hydrogen safety information dissemination tool.
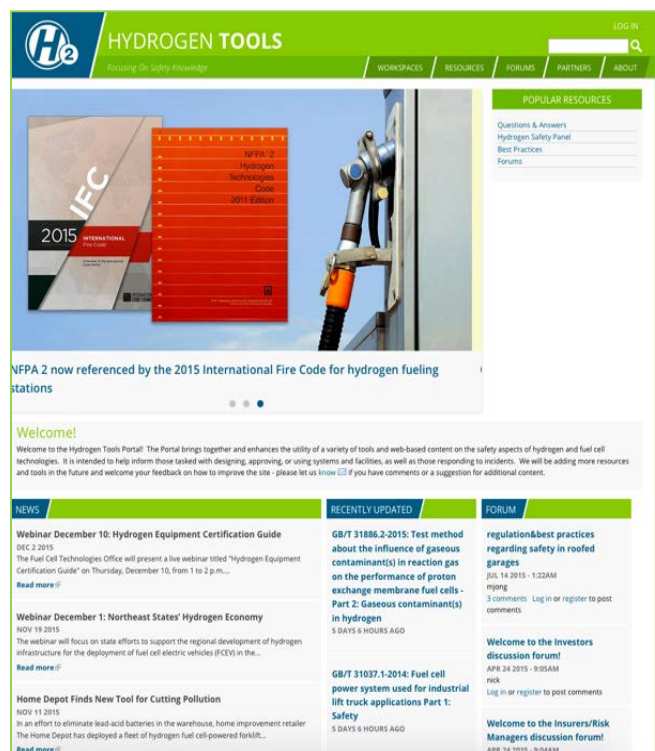

Figure 1. Hydrogen Tools Portal integrates safety knowledge resources into a single website (http://h2tools.org).

Grid Interaction

AC Level 2 Conductive Charging Interoperability Testing

Testing determined the interoperability of plug-in electric vehicles and electric vehicle supply equipment pairs, to ensure any plug-in electric vehicle can charge at any public SAE-compliant AC Level 2 charger.

Idaho National Laboratory and Intertek Center for the Evaluation of Clean Energy Technology

Idaho National Laboratory's (INL) field use of alternating current (AC) Level 2 (208-240 volt) electric vehicle supply equipment (EVSE) to recharge plug-in electric vehicles (PEVs) identified possible incompatibility and safety issues, and the occasional inability of some PEVs to fully charge.

Based on industry feedback, a mechanical and grid-event test project (see Figure 1) was launched to quantify interoperability issues. Results were provided to PEV and EVSE original equipment manufacturers (OEMs), and SAE for resolution. Researchers sought participation from as many PEV and EVSE OEMs as possible. Fourteen PEVs (12 OEMs) and 14 EVSE (12 OEMs) were included to evaluate the interoperability of various pairs of PEV-EVSE. Testing also evaluated the SAE J2953™ standard for PEV-EVSE interoperability and if test modifications were needed. Testing was conducted with SAE participation as part of INL's management of, and Intertek's testing activities for, the U.S. Department of Energy's Advanced Vehicle Testing Activity. Argonne National Laboratory provided testing software and most of the testing hardware.

Nearly 2,500 tests were conducted on various PEV-EVSE pairs (see Figure 2). The results were categorized either as no failures, soft failures, or complete charging failures. Individual OEMs were given in-depth test results and only the collective anonymized results were published (http://avt.inel.gov/pdf/evse/AVTEInteroperability Project-Phase1FinalReport.pdf). Observations made during testing were included for discussion within the SAE J2953™ committee and to provide information for those interested in more testing details.

Future interoperability testing is planned. Direct current fast chargers and wireless power transfer systems will be examined. This work is expected to be undertaken in calendar year 2016.

Figure 1. Testing data collection setup for one vehicle and EVSE pair.

Figure 2. Testing area, and the EVSE and one vehicle in testing.

Electric Vehicles Roll with Grid Modernization

Six U.S. Department of Energy national laboratories collaboratively developed the Electric Vehicle Smart Grid Requirements and Opportunities Report, which lays the foundation for key research initiatives that will make electric vehicles an integral part of grid modernization initiatives.

National Renewable Energy Laboratory

Plug-in electric vehicles (PEVs) continue to grow in popularity and present a risk and an opportunity to electricity grid operations. The U.S. Department of Energy (DOE) initiated a collaborative working group to develop a guidance document outlining the current state of PEV integration with the future smart grid, as well as challenges and barriers.[1] The group includes experts from the National Renewable Energy Laboratory (NREL), Argonne National Laboratory (ANL), Idaho National Laboratory (INL), Oak Ridge National Laboratory (ORNL), Lawrence Berkeley National Laboratory (LBNL), and Pacific Northwest National Laboratory (PNNL) (see Figure 1). The document is intended to guide the development of Vehicle Technologies Office-specific research topics that are part of DOE's Grid Modernization Initiative.

Objectives of the Grid Modernization Initiative include reducing the economic cost of power outages by 10% by 2025, decreasing cost of reserve margins by 33% by 2025 while maintaining reliability, and decreasing the net integration costs of distributed energy resources by 50% 2025.

The report discusses vehicle grid integration (VGI) scenarios, and summarizes current efforts to create foundational interface standards. The report highlights technology demonstrations. Data is relied upon to discuss the magnitude and variability of PEVs as a grid resource. The report considers simulation tools that can be used to explore VGI applications offering customer value. The team summarized the requirements and potential action items that would support greater VGI adoption. California agencies highlighted the multi-lab project output as critically related to their VGI roadmap.

Essential areas for further research and development include grid interactive vehicle systems simulation tools; hardware component and control architecture development and testing, including hardware in the loop; and market structure evolution and utility engagement.

DOE Laboratory	Core EV Grid Modernization Expertise
ANL	Standards development; component testing; hardware in the loop; embedded controls; Electric Vehicle (EV) Smart Grid Interoperability Center.
INL	Large-scale data collection and analysis; real-time power systems simulation and testing; technology characterization; cyber security.
LBNL	Optimization and controls; grid markets; systems simulation of EV loads; vehicle-to-grid pilot demonstrations.
NREL	Renewables integration; bi-directional power flow; charge management systems; MW-scale power system integration testing facilities.
ORNL	Power electronics design; vehicle-to-grid and wireless power transfer; buildings integration.
PNNL	Buildings integration; VOLTTRON software for component collaboration; smart charging systems valuation; grid modeling.

Figure 1. Summary of DOE national laboratory EV grid expertise contributed to report.

---

[1] Markel, T., et. al. (2015). "Multi-Lab EV Smart Grid Integration Requirements Study: Providing Guidance on Technology Development and Demonstration." http://www.nrel.gov/ docs/fy15osti/63963.pdf.

Hydrogen Storage

Adsorption-Based Hydrogen Storage Systems Validated

The Hydrogen Storage Engineering Center of Excellence evaluated and validated novel design concepts via the assembly and testing of sub-scale prototypes.

Hydrogen Storage Engineering Center of Excellence

As a culmination of the Hydrogen Storage Engineering Center of Excellence (HSECoE)[1], novel adsorbent-based hydrogen storage system designs were demonstrated as subscale prototypes. These prototypes allowed for assessment of sub-system and full-scale performance, which is relevant to innovative thermal management concepts. Prototype testing is critical to identifying ways to improve the predictive capability of the models, resulting in component designs that approach the U.S. DRIVE hydrogen storage targets.

HSECoE systematically assessed the performance of two prototype systems by characterizing multiple system functions, including material performance, internal heat exchanger capability, and thermal management. This approach confirmed the robustness of the metal organic framework (MOF)-5 adsorbent material using real-world fueling cycles and impurity levels allowed by hydrogen fuel standards.

HSECoE determined the thermal conductivity of MOF-5 as a function of the hydrogen operating pressure and system temperature for the first time, allowing for comparative assessments of innovative heat exchanger designs. The heat exchanger is a key component of the sorbent-based hydrogen storage system, as its performance dictates the fill time. One heat exchanging concept used convective cooling through hexagonal cells (HexCell) filled with adsorbent powder. The other concept employed micro-channel plates as part of a modular adsorption tank insert (MATI) with compacted sorbent. The HexCell prototype (see Figure 1) was shown to be capable of achieving the targeted operating temperature during a three-minute refuel

event. The team also confirmed the robustness of the MATI system through repeated temperature and pressure cycling.

Also, HSECoE tested a novel thermal management system to directly cool the walls of the pressure vessel. This concept employed a liquid nitrogen cooling jacket and confirmed model predictions that indicated an order of magnitude reduction in coolant requirements compared to prior designs.

These prototypes validated the models HSECoE designed and will help accelerate the development of efficient, material-based hydrogen storage systems.
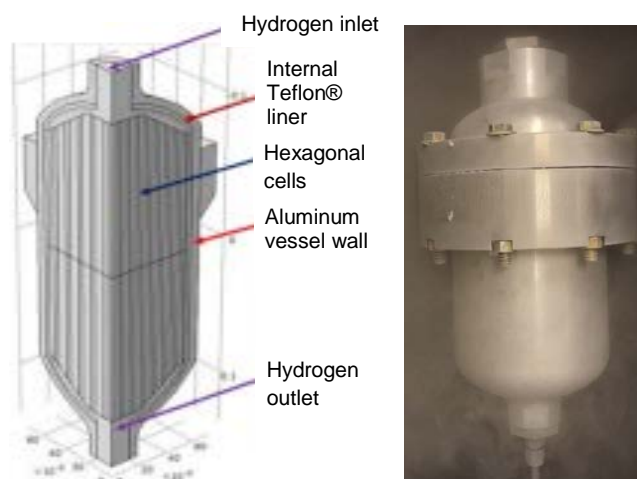

Hydrogen inlet
Internal Teflon® liner
Hexagonal cells
Aluminum vessel wall
Hydrogen outlet

Figure 1. HexCell subscale adsorbent prototype was designed, built, and evaluated by the HSECoE for comparison against predictive models.

---

[1] HSECoE is led by Savannah River National Laboratory with ten industry, university, and national laboratory partners.

Lower-Cost Hydrogen Storage System

700 bar Type IV compressed hydrogen storage system cost is projected to be 12% lower than the 2013 baseline.

Strategic Analysis, Inc., Oak Ridge National Laboratory, and Pacific Northwest National Laboratory

Strategic Analysis, Inc. (SA) performed a cost analysis that projected a 12% net reduction in the cost of a 700 bar type IV (polymer liner and carbon fiber (CF) composite overwrap) onboard hydrogen storage system from the previous 2013 baseline estimate. As illustrated in Figure 1, the high volume cost was reduced from $16.8/kWh in 2013 to $14.8/kWh in 2015. These savings were achieved based on material and technology advancements identified by Oak Ridge National Laboratory (ORNL), Pacific Northwest National Laboratory (PNNL), and SA.

The CF composite overwrap (i.e., CF and resin matrix) accounts for more than half of the projected high volume cost of the compressed hydrogen storage system, and the cost of the CF precursor accounts for more than half of the cost of the CF. ORNL led a team that developed a lower cost polyacyrlonitrile-methacrylate (PAN-MA) precursor fiber produced using high volume textile manufacturing processes. The CF made using this new precursor fiber process is projected to be 18% less expensive than CF made using conventional lower volume CF manufacturing processes while maintaining the same mechanical properties. PNNL led a parallel effort that identified an alternative lower density, lower cost resin, resulting in a lower weight CF composite with improved mechanical properties over the conventional epoxy resin. Based on technology advancements developed by the ORNL and PNNL teams, the resulting cost reduction for onboard hydrogen storage system is 11% and 4%, respectively.

Balance of plant (BOP) components account for nearly a quarter of the high-pressure storage tank system cost. SA identified cost savings of 9% by applying a design for manufacturing and assembly approach along with integration of components based on input from the industry. This approach led to a reduction in the total number of parts and fittings, which reduced the BOP cost.

In addition to the cost reductions noted above, SA worked with tank manufacturers to reevaluate the original assumptions. To ensure storage system manufacturing reliability at high volumes, some design changes were made due to difficulty in reproducibility experienced using fiber placement (dollies) on the dome ends of the pressure vessel as well as variation in fiber performance. In total, the revised cost analysis resulted in a 12% reduction even with allowances made for improved manufacturing reliability.
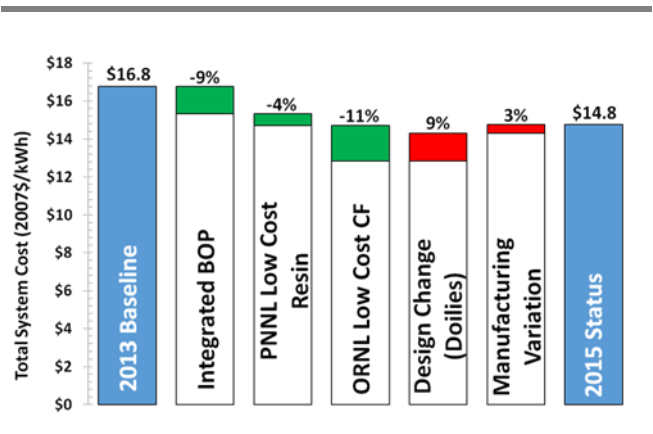
Figure 1. Breakdown of incremental cost changes for the 2015 type IV compressed hydrogen storage system against the 2013 baseline system (assumes 500,000 units per year).

FUELS

Fuel Pathways Integration

Hydrogen Fuel Pathway Analysis

In the modeled scenario, hydrogen produced via emerging renewable and lower-carbon pathways is expected to have dispensed hydrogen costs exceeding the U.S. Department of Energy's $4/kg target, indicating the need for further research & development.

Fuel Pathways Integration Technical Team

The Fuel Pathway Integration Technical Team (FPITT) provided feedback to the U.S. Department of Energy's (DOE) preliminary evaluation of the cost (including the cost of hydrogen (H_2) infrastructure) and lifecycle greenhouse gas (GHG) emissions performance of four emerging-technology H_2 production, delivery, and distribution pathways. This pathway assessment focused on the potential of several emerging H_2 production technologies for reducing GHG emissions and increasing the use of renewable energy resources in the production of H_2 fuel. Modeled pathways included pipeline delivery and 700 bar dispensing of H_2 produced via natural gas reformation utilizing carbon capture and sequestration (CCS), and H_2 produced from photo-biological, photo-electrochemical and solar thermo-chemical processes.

The emerging-technology H_2 pathway assessment complements DOE's previous evaluation of current- and advanced-technology pathways, investigating the costs, energy use, and GHG emissions predicted to result from emerging H_2 technologies that could be available in the 2025-2030 timeframe. As with the previous assessment, FPITT members reviewed DOE's analysis methods, assumptions, and data.

The previous analysis of advanced-technology H_2 pathways found that only the distributed production of H_2 via natural gas reformation was expected to meet DOE's $4/kg dispensed H_2 cost target (untaxed).[1] Including costs for H_2 production, delivery, and refueling station compression, storage, and dispensing (CSD), the 2015 analysis of

emerging-technology H_2 pathways found that none of the pathways studied are expected to meet the $4/kg-$H_2$ cost target based on the current technology status, indicating the need for further research and development. (Publication of GHG emissions estimates for these pathways is awaiting further modeling; publication of emerging-technology pathway costs is expected in fiscal year 2016).

DOE's emerging-technology pathways evaluation was conducted using its publicly available models, with costs reported in 2007 U.S. dollars.[2] Figure 1 shows preliminary levelized costs of dispensed H^2 for the pathways analyzed.
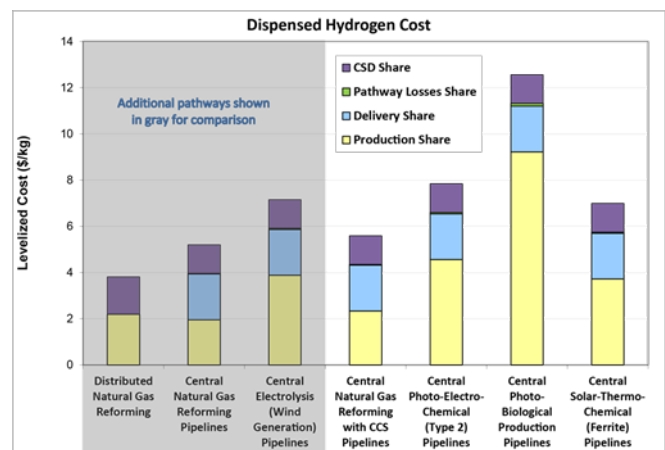

Figure 1. Preliminary dispensed H_2 levelized cost (including cost of infrastructure) for four emerging-technology pathways.

---

[1] See Ramsden, T., "Pathway Analysis: Projected Cost, Life-Cycle Energy Use and Emissions of Future Hydrogen Technologies," *DOE Hydrogen and Fuel Cells Program: 2014 Annual Progress Report.* U.S. DOE, Nov. 2014. DOE/GO-102014-4504.

[2] The analysis uses a version of DOE's Hydrogen Macro-System Model that incorporates the latest component models as of October 2014: H2A Version 3 (2012), HDSAM Version 2.3 (2012), GREET 1 (2014) and GREET 2 (2014).

Marginal Abatement Cost of Carbon

Analysis compares cost and magnitude of greenhouse gas emission reductions for different vehicle technologies and fuel pathways compared to a baseline mid-sized gasoline vehicle on an avoided emissions basis.

Fuel Pathways Integration Technical Team

The Fuel Pathways Integration Technical Team completed an analysis to compare cost and magnitude of greenhouse gas (GHG) emission reductions for different vehicle technologies and fuel pathways, compared to a baseline mid-size gasoline vehicle, on an avoided emissions basis.[1]

The vehicle technologies selected for this analysis included battery electric vehicle (BEV), plug-in hybrid (PHEV), compressed natural gas (CNG), fuel cell hybrid electric vehicle (FCHEV), diesel, flex-fuel (ethanol E85), liquefied petroleum gas (LPG), and gasoline (E10). Technology choices and assumptions align with pathways analyzed by the U.S. DRIVE Cradle-to-Grave working group. The analysis includes short- and long-term technology perspectives to assess changes once newer technologies are produced "at scale."

Figure 1 shows the results of the analysis for the near-term case with uncertainty ranges. The horizontal axis indicates tonnes of carbon dioxide equivalent (CO_2e) saved during the lifetime of the vehicle compared to a baseline technology, and the vertical axis shows additional cost paid per tonne of avoided CO_2e compared to the same baseline in log scale.[2] In this case, the BEV210 vehicle is expected to have the highest abatement cost.

Figure 2 shows the cost of avoided emissions for some of the pathways of the hypothetical long-term case (potential technology adoption in the 2025-2030 timeframe). In this case, the diesel fatty-acid methyl ester (FAME) pathway has the highest cost of abatement, followed by BEV210 powered by wind electricity and LPG.

Figure 1. Graphical representation of results for the near-term scenario with uncertainty ranges relative to a conventional gasoline baseline. Note: The results are presented in log scale.
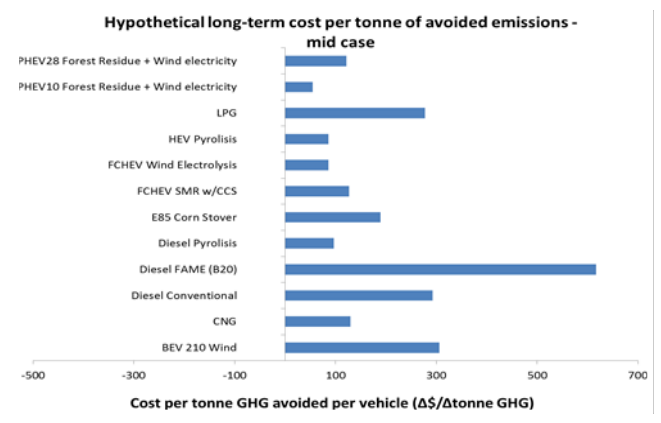
Figure 2. Graphical representation of results for the hypothetical future scenario relative to a conventional gasoline baseline.

---

[1] Avoided GHG emissions are defined as the difference between the GHG emissions calculated for a given alternative vehicle-fuel combination and those that would have been released by a mid-size gasoline-fueled internal combustion engine vehicle.
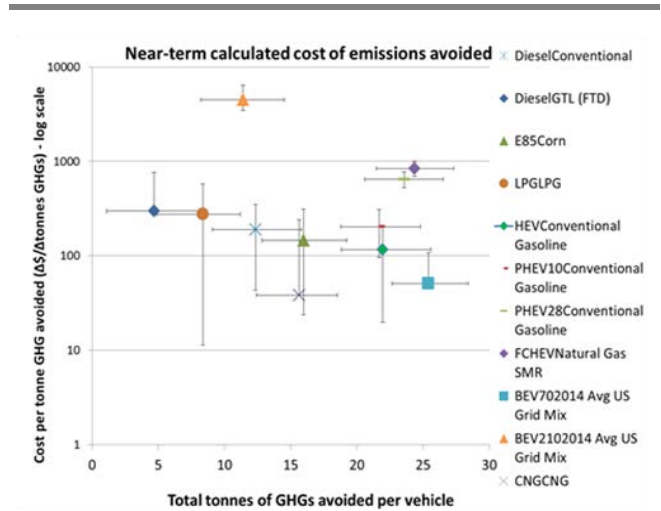
[2] CO_2e is a measure used to compare the emissions from various greenhouse gases based upon their global warming potential.

Hydrogen Delivery

Hydrogen Delivery Scenario Analysis Model Version 3.0

Model provides updated cost and performance estimates of current and future hydrogen delivery and refueling technologies.

Argonne National Laboratory

Argonne National Laboratory (ANL) has released version 3.0 of its Hydrogen Delivery Scenario Analysis Model (HDSAM). HDSAM is a bottom-up model that calculates the levelized cost of hydrogen delivery and dispensing in user-specified scenarios. Hydrogen delivery is defined as the entire process of moving hydrogen from the gate of a central production plant to a vehicle's tank. Thus, delivery includes all transport, storage, and conditioning steps (e.g., compression and liquefaction) from the outlet of a centralized hydrogen-production facility to a refueling station that dispenses hydrogen. Researchers and government personnel regularly use the model to evaluate the impacts of technologies and R&D strategies.

HDSAM uses engineering principles to optimize delivery facility design, such as refueling stations. Specifying key assumptions (e.g., station type and size) allows the model to calculate the most cost-effective facility solution (e.g., compressors, pipelines, terminals and pipelines). The model estimates the cost of the designed pathway and completes a discounted cash flow analysis of the pathway over 30 years. Key outputs of the model include the levelized cost of hydrogen, annual cash flows from the station, capital and operating costs of the delivery facilities, land area requirements, energy consumption and greenhouse gas emissions (see Figure 1). The model and associated documentation are publicly available.[1]

In HDSAM 3.0, cost equations and technologies have been updated to reflect the current market. Compression and station refrigeration technologies have both been updated to reflect current practice. The costs of key equipment, such as liquefiers, liquid pumps, dispensers, and storage, have been updated with industry input. HDSAM's projections were compared to real-world stations using applications for funding that station developers submitted to the California Energy Commission. HDSAM's capital cost projections for three real-world stations were within 15% of developers' budgeted values.

HDSAM 3.0 allows users to project the impacts of market penetration on the costs of hydrogen delivery equipment. Projections are based on expected cost reductions due to advancements in manufacturing capabilities and economies of scale. Additionally, the model allows users to input a station's annual utilization rate for 30 years, the most significant variable affecting station economics in the early market.

The model estimates that hydrogen delivery cost can reach $10-$15 per kg of hydrogen in early markets where economies of scale are not realized and the infrastructure is under-utilized. The cost to deliver and dispense hydrogen for 700 bar hydrogen vehicles in a mature market is estimated at $3-$4/kg.
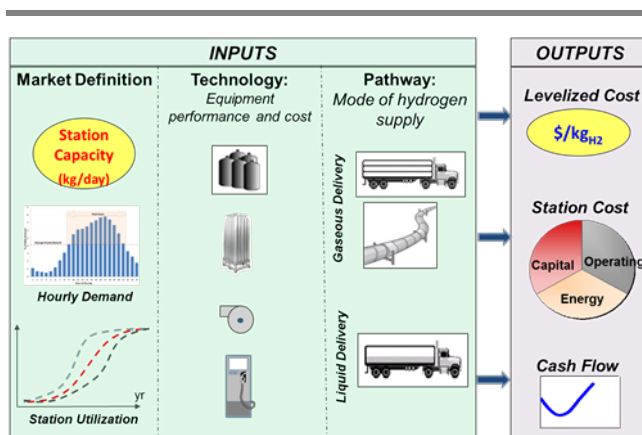

Figure 1. Inputs and outputs of HDSAM tool.

---

[1] http://www.hydrogen.energy.gov/h2a_delivery.html.

40% Capital Cost Reduction of 430 bar Stationary Storage

A low-cost steel concrete composite vessel was developed for stationary hydrogen storage that offers significant cost reduction over the standard steel vessels.

Oak Ridge National Laboratory

Through the design of a steel concrete composite vessel (SCCV), the capital cost of 430 bar stationary hydrogen storage has been reduced by 40% from the 2011 figure of $1,100/kg, to $660/kg. The 90-kg prototype developed by Oak Ridge National Laboratory (ORNL), which is shown in Figure 1, was built according to the requirements of the ASME Boiler and Pressure Vessel Code, and passed testing per ASME standards for safety and construction, resulting in certification for 430 bar service.

ORNL's SCCV reduces the cost of hydrogen storage by using concrete in lieu of steel for the outer vessel layers. The SCCV design combines a thin stainless steel liner with load-bearing low-alloy structural steels layers and an outer layer of pre-stressed concrete. The pre-stressed concrete bears 50% of the vessel's structural load.

430-bar hydrogen storage vessels can be used for low- and medium-pressure buffer storage at tube trailers loading terminals and at refueling stations. The SCCV design is guided by ORNL's 2012 manufacturing cost analysis, which indicated that a 430-bar hydrogen storage vessel would cost about $710/gge ($660 in 2007 dollars). This cost would decrease by about 4% if friction stir welding were used to weld the layers.

This capital cost reduction results in an overall pathway cost reduction of up to $0.50 per kg. The Hydrogen Delivery Scenario Analysis Model (HDSAM) V3.0 was used to simulate the tube-trailer delivery pathway with standard assumptions[1] and 2014 cost of 430-bar storage, resulting in a levelized cost of delivery and dispensing of $4.30/gge.[2] When the cost of hydrogen storage is changed to $660/gge (to represent the SCCV), the cost of delivery and dispensing is $3.80/gge. The SCCV capital cost is therefore projected to generate $0.50/gge in cost savings.

ORNL is currently optimizing the SCCV design so that it can also be used for stations' high-pressure storage requirements. The 875-bar storage vessel in development will utilize more rebar and thicker stainless steel than the 430-bar vessel.

Figure 1. The low-cost steel concrete composite hydrogen storage vessel ORNL developed.

[1] Standard assumptions that represent a mature fuel cell electric vehicle market are detailed in DOE Record 13013.

[2] One gallon of gasoline equivalent (gge) is approximately equal to one kg of hydrogen on an energy basis.

Codification of Fiber Reinforced Polymer and High-Strength Steel for Hydrogen Pipelines

Low-cost alternatives to traditional steel pipelines have passed the ASME B31.12 Code Committee.

Savannah River National Laboratory and Sandia National Laboratories

Savannah River National Laboratory (SRNL) has proposed modifications to the ASME B31.12 design code for Hydrogen Piping and Pipelines to allow the use of fiber reinforced polymer (FRP) in the construction of hydrogen (H_2) pipelines (see Figure 1). The ASME B31.12 Code Committee has passed the modifications, which the B31 Standards Committee is now considering. Use of FRP for a 1" distribution line is projected to result in $0.14/gge cost savings over steel, representing a greater than 25% reduction in installation cost of the line. Moreover, research completed by Sandia National Laboratories (SNL) has been leveraged to propose additional modifications to ASME B31.12 to facilitate use of higher-strength steels.

FRP is more advantageous than steel in pipeline construction primarily because it is less expensive to install. While steel pipe must be delivered to a construction site in lengths of about 80' or less, FRP can be delivered in 0.5-mile long spools or even manufactured onsite in lengths of 2-3 miles. As a result, less heavy-duty equipment and manpower is required to join segments of pipe together. To determine the suitability of FRP for H_2 service, SRNL measured key mechanical properties of commercially available FRP pipe, including fatigue resistance, hydrostatic strength, stress rupture time, permeation rates, anticipated life in H_2 (via accelerated life testing), flaw tolerance, and resistance to common environmental stressors. The experimental data formed the basis for the proposed inclusion of FRP in the ASME B31.12 code for H_2 service at 1500 psi with a 50-year life.

Additionally, in fiscal year 2015 SNL completed experimentation on X65 steel in H_2, and combined the resulting data with several previous years' data from both SNL and the National Institute of Standards and Technology (NIST) to show that higher-strength steels (i.e., X65-X80) are not necessarily less resistant to H_2 assisted fatigue crack growth than lower strength steels (i.e., X52) under the service conditions expected in pipelines (load ratios of 0.5, and pressures of at least 1500 psi). NIST used these data to propose modifications to ASME B31.12 that reduce the thickness requirements (and thereby the cost) of using X70 steel in 1500-psi H_2 pipelines. Using X70 rather than X52 in compliance with the modified code can lower the cost of pipeline material by up to 25%.

Recent research indicates that the resistance of steel to H_2 embrittlement more closely depends on its microstructure than its mechanical strength. Traditionally, however, high-strength steels were thought to be less resistant to embrittlement than low-strength steels. As a result, ASME B31.12 formerly imposed "material performance factors" on the use of high-strength steels in H_2 service that effectively required H_2 pipelines to be thicker if they were made of X70 rather than X52 in many service and design conditions. The proposed modifications to the ASME B31.12 code will reduce these material performance factors, thereby allowing the use of thinner steels in pipeline construction. A reduction in the quantity of steel used (i.e., "thinning") will drive the cost of H_2 delivery closer to the $2.00/gge ultimate H_2 cost target.

Figure 1. Installation of a spool of FRP.

Hydrogen Production

Low Precious Group Metal Loaded Catalysts/Electrodes for Hydrogen Production by Water Electrolysis

Proton OnSite successfully demonstrated the reduction of the precious metal group metal content of its electrolyzer-cathodes by an order of magnitude without sacrificing electrochemical performance.

Proton OnSite

Proton OnSite, working with Brookhaven National Laboratory (BNL), has reduced the precious group metal (PGM) catalyst loadings in polymer electrolyte membrane (PEM) electrolyzer electrodes by an order of magnitude to levels comparable to state-of-the-art PEM fuel cells. This achievement, leveraging an electrocatalysis approach originally investigated for lowering PGM loading in PEM fuel cell cathodes, combines an adaptation of BNL's core shell catalyst technology for electrolyzer use with Proton's scalable manufacturing process for effectively synthesizing and depositing the nanoparticle catalysts. It is estimated that decreasing the electrolyzer cathode PGM loading by an order of magnitude, in combination with manufacturing developments, will decrease the electrolyzer stack capital costs by approximately 18%.

PEM electrolyzers have been slow to adopt many of the advancements made in their PEM fuel cell counterparts. For example, the electrode catalyst loadings in today's PEM electrolyzers are typically higher than those in PEM fuel cells by at least a factor of five. One historical reason for this lag is that electrolyzers were originally developed for life support applications in space and on submarines, requiring ultimate dependability achieved through over-engineered stack designs, including high catalyst loadings. Also, achieving uniform catalyst distribution across the electrodes using the legacy deposition processes inherently requires substantial catalyst loadings.

Proton and BNL targeted the cathode, or hydrogen electrode for the electrolysis cell, for initial demonstration. Researchers used an environmentally friendly ethanol-based process developed at BNL to synthesize atomically well-designed core-shell nanocatalysts, which consist of a less expensive core metal covered by a more

expensive, catalytically active shell material. These nanocatalyst particles were integrated with carbon supports and deposited on a microporous layer in a test cathode at PGM loadings of <0.15 mg/cm^2. Performance tracked very well with Proton's baseline electrode, which had an order of magnitude higher PGM loading (Figure 1). The new catalyst demonstrated stable performance in a 500 hour test showing that even though significantly less catalyst is used, good performance life is still achievable.

Proton successfully transferred manufacturing of the core shell catalysts to its facilities at a scale practical for Proton's current fabrication processes. The catalyst deposition method was transitioned from a manual process to an automated ultrasonic printing process, which has proven effective for uniformly dispersing the core shell catalysts at low loadings.
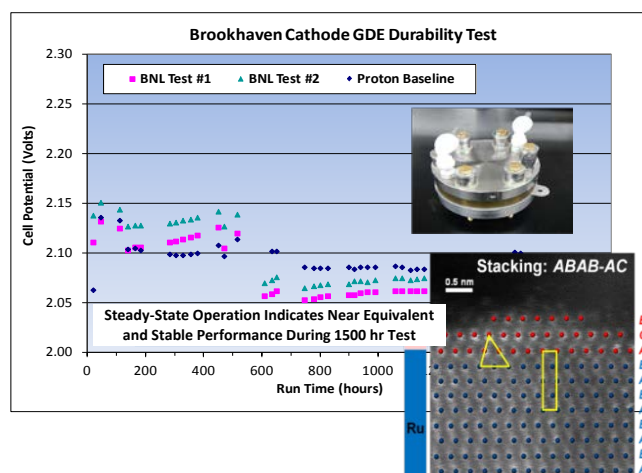

Figure 1. Core shell catalyst structure and performance data.

Techno-Economic Analysis of Hydrogen Production from Solid Oxide Electrolysis

New analysis highlights the potential for centralized hydrogen production from highly efficient solid oxide electrolysis.

Strategic Analysis, Inc.

New cost projections are now available for hydrogen (H_2) production from solid oxide electrolysis (SOEC). This technology's high operating temperature enables operation at very high electrical efficiencies (approaching 100%) while maintaining high H_2 production rates, allowing an electricity cost savings of greater than $1/kg H_2 compared to low-temperature electrolysis H_2 production. Laboratory-scale SOEC technology has shown significant performance potential, including advances achieved with U.S. Department of Energy (DOE) support, with electrical efficiencies approaching 100% (lower heating value of H_2). The results of the new case studies will guide research and development efforts to further the goals of low-cost H_2 production.

Strategic Analysis, Inc. and the National Renewable Energy Laboratory prepared case studies of H_2 production costs through SOEC water splitting using Hydrogen Production Analysis Model (H2A) Version 3.1.[1] Six SOEC research organizations and developers provided input and vetted the results. The two cases evaluated are for centralized plants (100-500 metric tons H_2 per day) with a Current case based on 2014 lab-proven technology and a Future case based on expected technology advancements by 2025. Forecourt production (1-5 metric tons H_2/day) was not analyzed as SOEC technology is better suited for large, centralized production facilities. Researchers evaluated stack, balance-of-plant, indirect, replacement, decommissioning, operating & maintenance, and feedstock costs.

Recent H2A case studies on low-temperature polymer electrolyte membrane electrolysis have shown the electricity feedstock cost to contribute up to 75% of H_2 production cost, clearly indicating the benefit of increasing electrical efficiency. SOEC used in conjunction with high-temperature process heat offers the largest potential for cost effective H_2 production as some electrical energy can be replaced with generally less expensive thermal energy. Due to the lower electrical usage, the SOEC H2A case studies show the electricity cost contribution to the H_2 production cost to decrease by more than $1/kg H_2 compared to low-temperature electrolysis. Some of this cost saving is offset by the cost of the thermal energy required.

Based on a natural gas combustion system supplying the heat, the baseline H2A analysis results presented in Table 1 use a thermal energy cost of ~60% of the electricity cost. The "Free Heat" column assumes the availability of thermal energy (T~900°C) at no cost to provide a lower bound. To reach DOE's long-term H_2 production target of less than $2/kg H_2, further reductions in capital and electricity costs as well as improved durability are needed.

Case Study	Baseline ($/kg H_2)	"Free Heat" ($/kg H_2)
Central: Current Case	$4.95	$4.41
Future Case	$3.83	$3.33

Table 1. H_2 production high-volume cost projections for the SOEC cases.

---

[1] http://www.hydrogen.energy.gov/h2a_prod_studies.html.